

Over view of basic devices

- 3908 Review – illustrate with some of the concepts developed previously
 - PN diode (minority injection over a barrier)
 - BJT (minority diffusion based device)
 - MOS (majority drift based device)
- LED
- Solar Cells

Fig 6.1

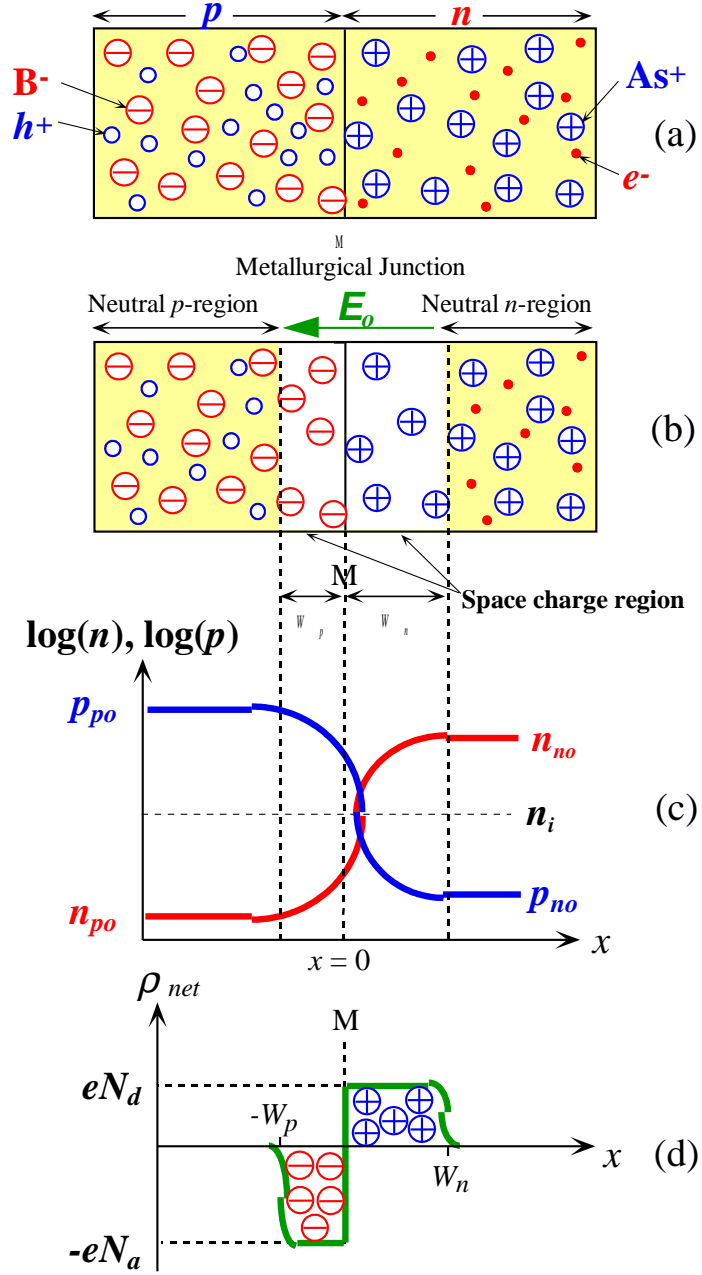
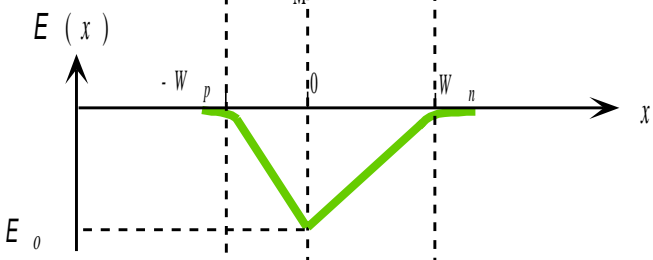
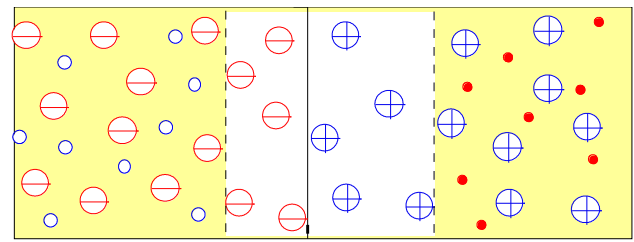
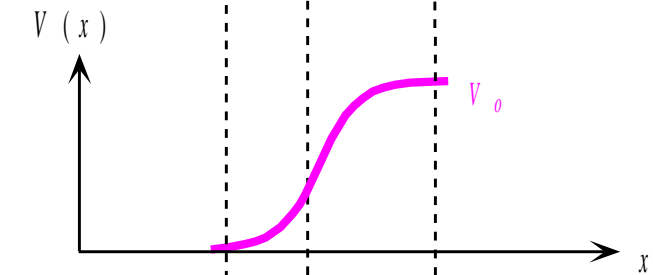


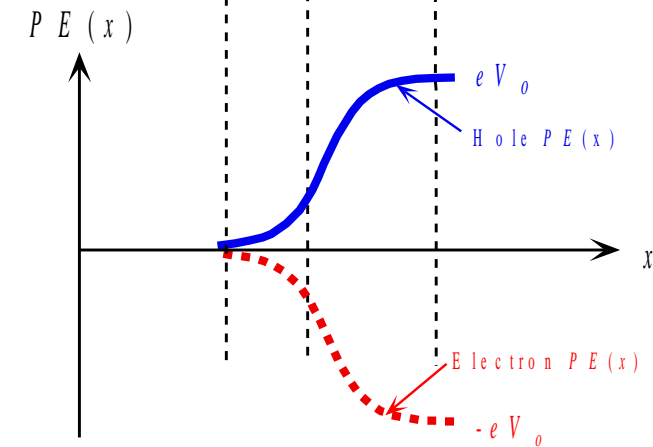
Fig 6.1
Properties of the pn junction



(e)



(f)



(g)

Fig 6.1

Ideal *pn* Junction

Acceptor concentration

Donor concentration

Depletion Widths

$$N_a W_p = N_d W_n$$

Field (E) and net space charge density

Net space charge density

$$\frac{d\mathcal{E}}{dx} = \frac{\rho_{\text{net}}(x)}{\epsilon}$$

Permittivity of the medium

Field in depletion region

$$\mathcal{E}(x) = \frac{1}{\epsilon} \int_{-W_p}^x \rho_{\text{net}}(x) dx$$

Electric Field

Ideal *pn* Junction

Built-in field

$$\mathcal{E}_o = -\frac{eN_d W_n}{\epsilon} \quad \text{where } \epsilon = \epsilon_o \epsilon_r$$

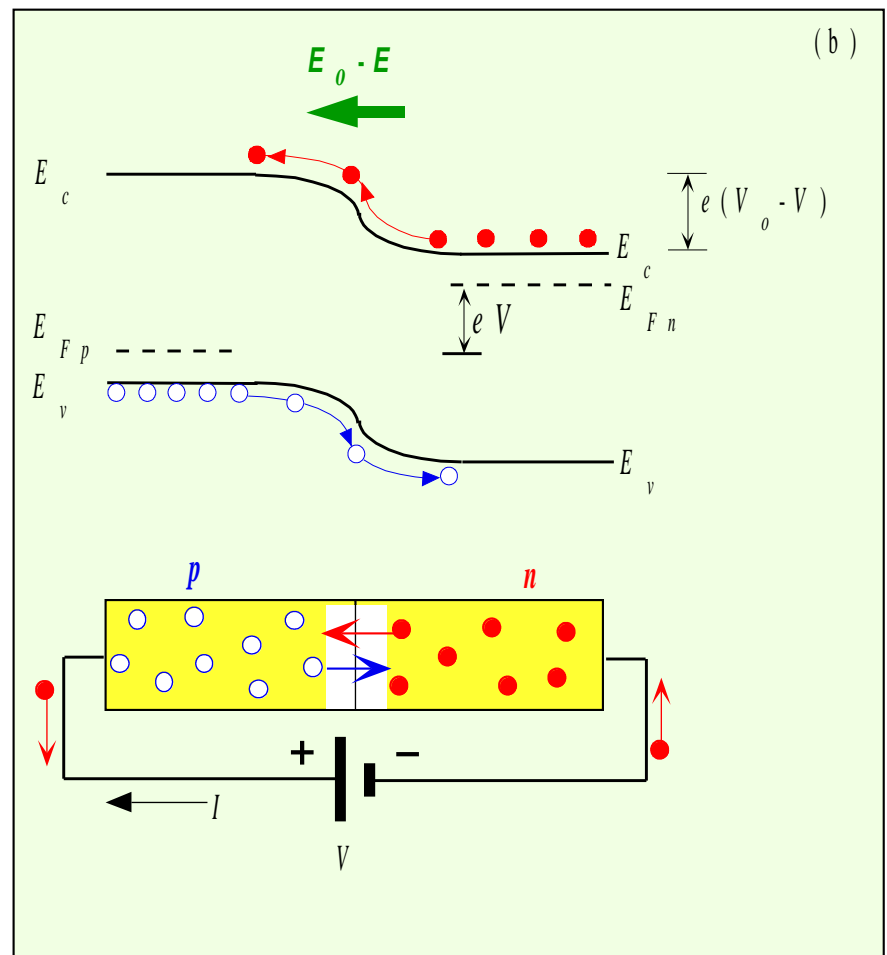
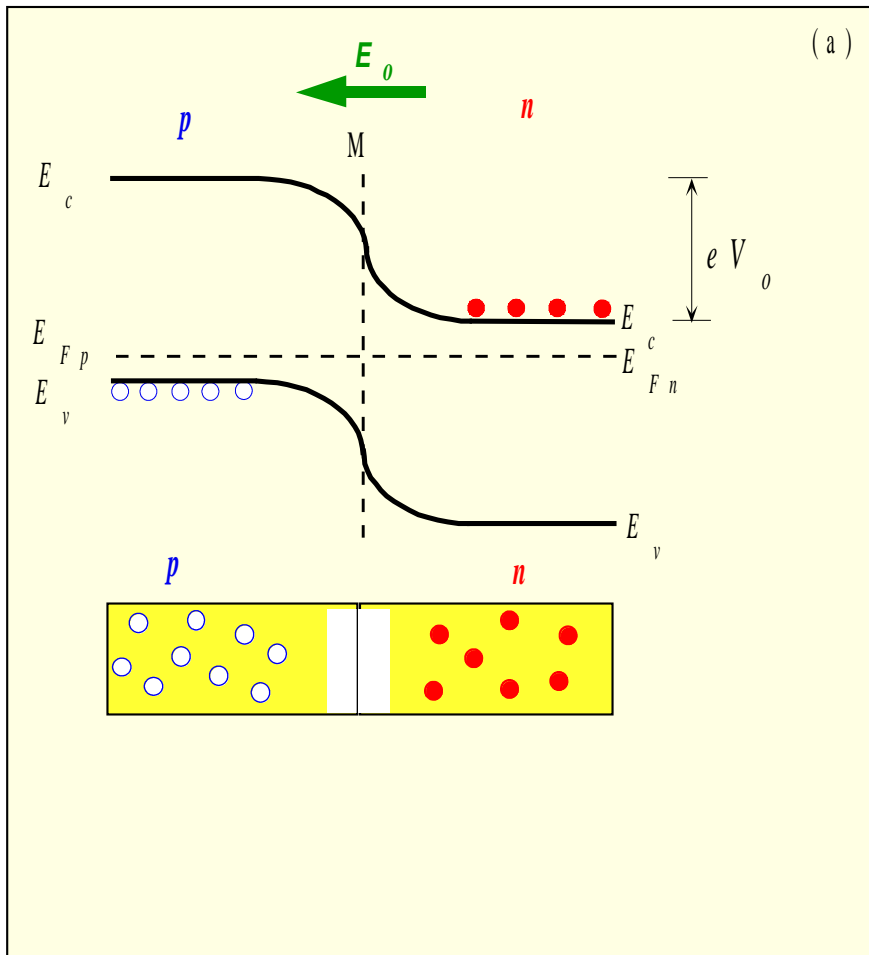
Built-in voltage

$$V_o = \frac{kT}{e} \ln\left(\frac{N_a N_d}{n_i^2}\right) \quad \text{where } n_i \text{ is the intrinsic concentration}$$

Depletion region width

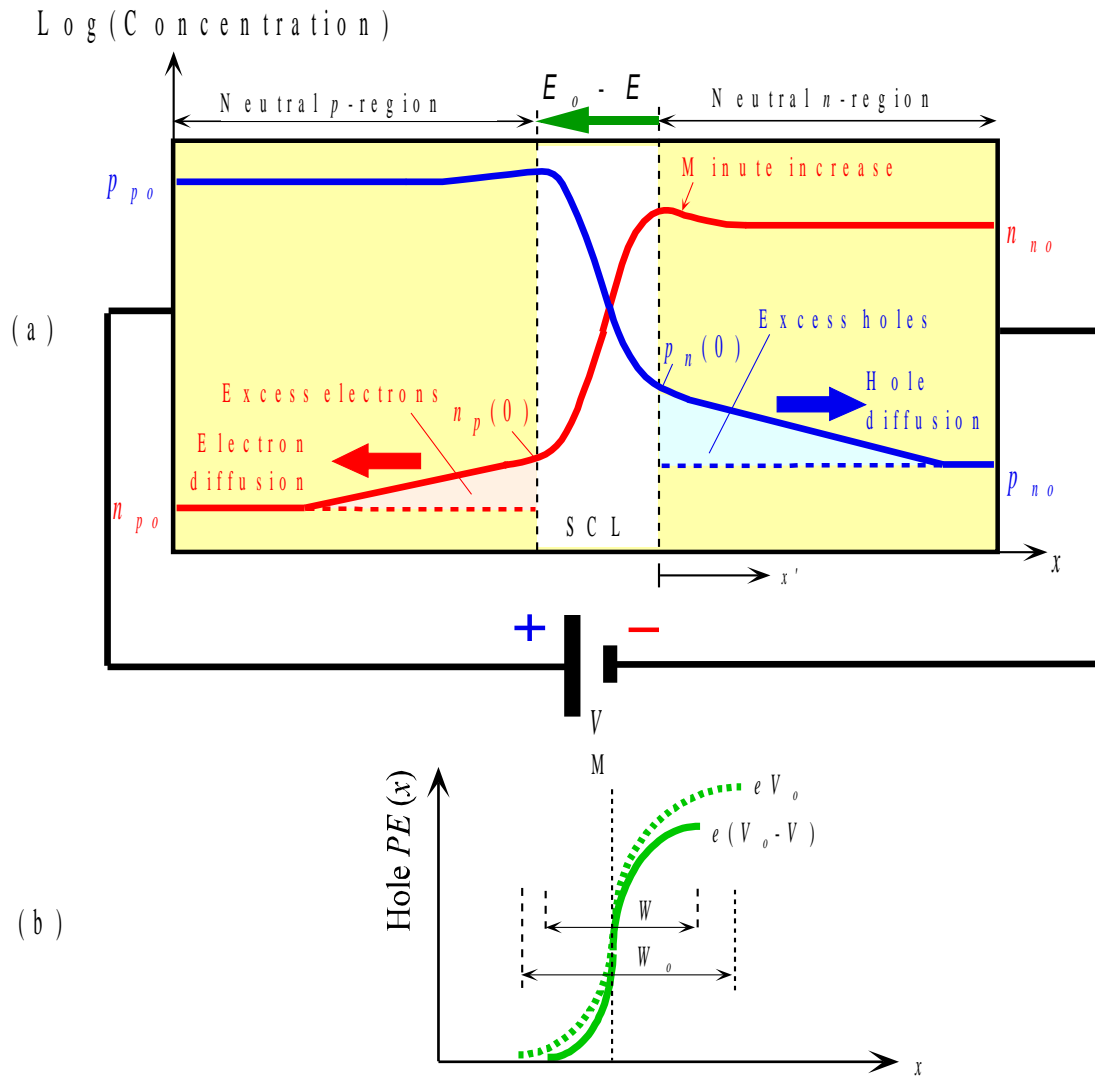
$$W_o = \left[\frac{2\epsilon(N_a + N_d)V_o}{eN_a N_d} \right]^{1/2}$$

where $W_o = W_n + W_p$ is the total width of the depletion region under a zero applied voltage



Energy band diagrams for a pn junction under (a) open circuit and (b) forward bias

Fig 6.11



Forward biased pn junction and the injection of minority carriers. (a) Carrier concentration profiles across the device under forward bias. (b) The hole potential energy with and without an applied bias. W is the width of the SCL with forward bias

Fig 6.2

Forward Bias: Diffusion Current

Law of the Junction: Minority Carrier Concentrations and Voltage

$$p_n(0) = p_{no} \exp\left(\frac{eV}{kT}\right)$$

$$n_p(0) = n_{po} \exp\left(\frac{eV}{kT}\right)$$

$p_n(0)$ is the hole concentration just outside the depletion region
on the n -side

$n_p(0)$ is the electron concentration just outside the depletion
region on the p -side

Forward Bias: Diffusion Current

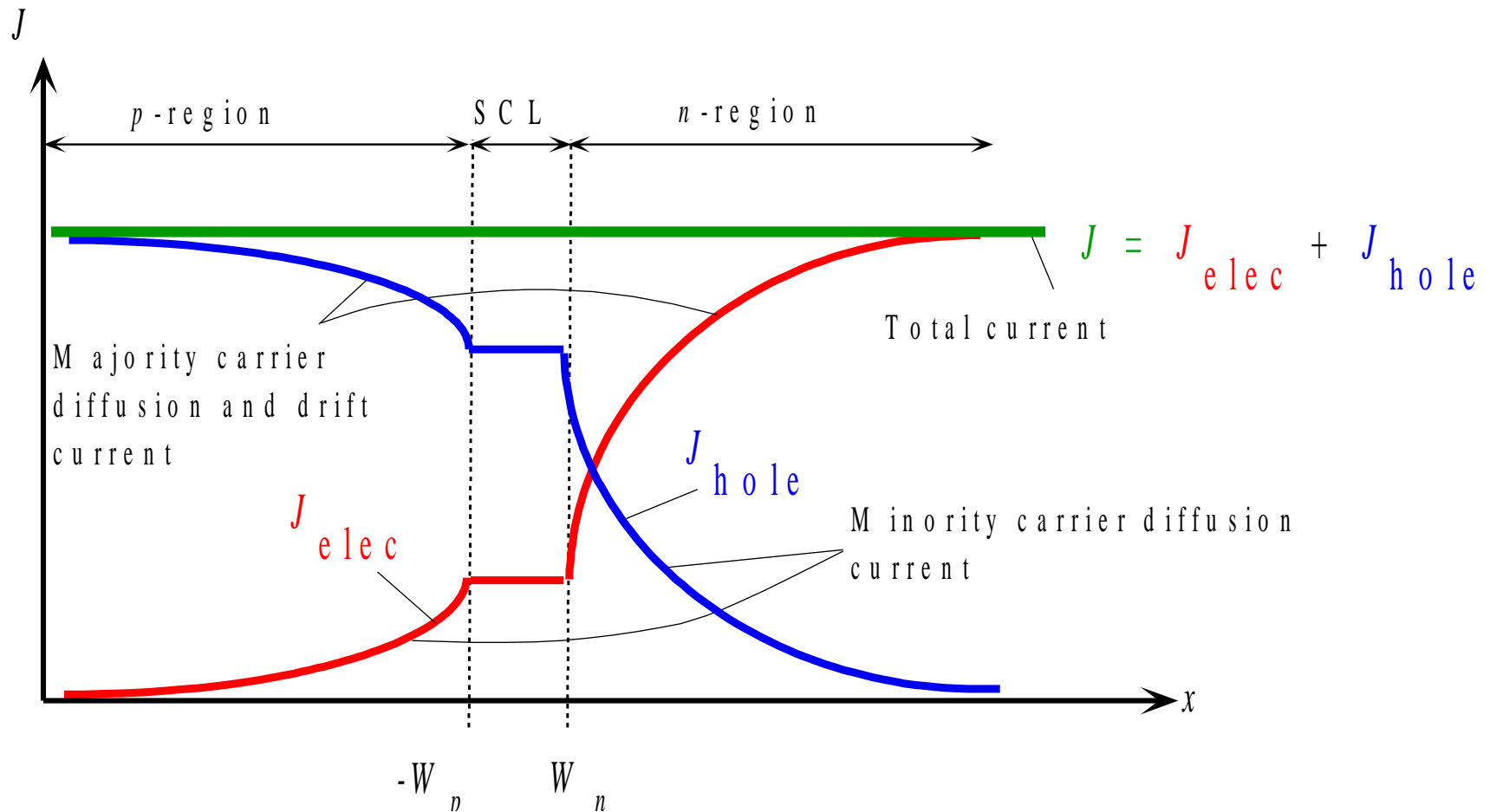
Excess minority carrier concentration profile

$$\Delta p_n(x') = \Delta p_n(0) \exp\left(-\frac{x'}{L_h}\right)$$

where L_h is the hole diffusion length, defined by $L_h = \sqrt{D_h \tau_h}$ in which τ_h is the mean hole recombination lifetime (minority carrier lifetime in the n -region).

Excess minority carrier concentration

$$\Delta p_n(x') = p_n(x') - p_{no}$$



The total current anywhere in the device is constant. Just outside the depletion region it is due to the diffusion of minority carriers.

Fig 6.3

Forward Bias: Diffusion Current

Hole diffusion current in n -side in the neutral region

$$J_{D,\text{hole}} = \left(\frac{eD_h n_i^2}{L_h N_d} \right) \left[\exp\left(\frac{eV}{kT} - 1 \right) \right]$$

There is a similar expression for the electron diffusion current density $J_{D,\text{elec}}$ in the p -region.

Forward Bias: Diffusion Current

Intrinsic concentration

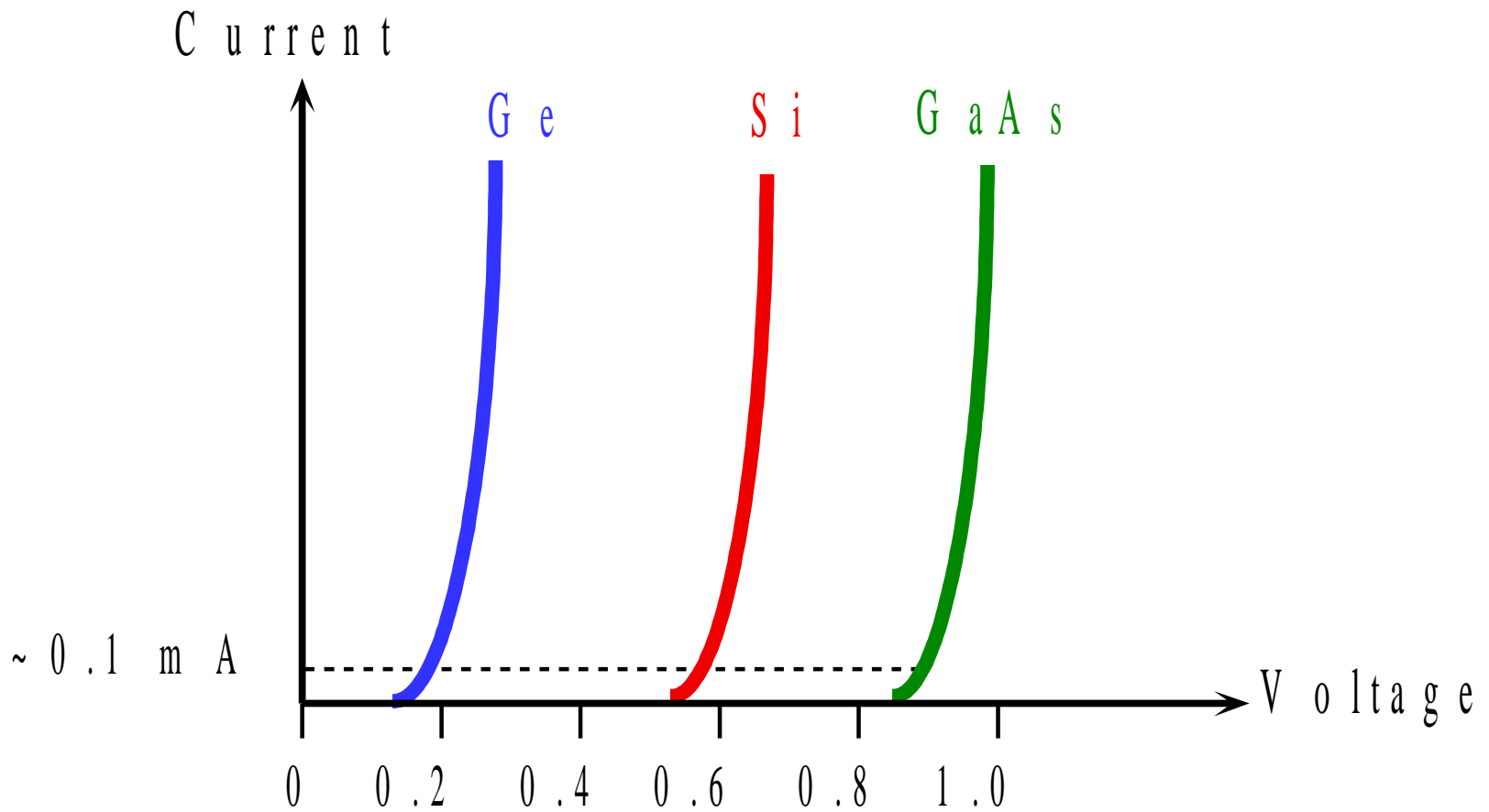
$$n_i^2 = (N_c N_v) \exp\left(-\frac{eV_g}{kT}\right)$$

where $V_g = E_g/e$ is the bandgap energy expressed in volts

$V_g = 0.67$ V for Ge, 1.1 V for Si, and 1.42 V for GaAs

$$J = J_{so} \exp\left(\frac{eV}{kT}\right) = C \exp\left(\frac{e(V - V_g)}{kT}\right) \quad V > kT/e$$

We can plot I vs. V for Ge, Si and Ge



Schematic sketch of the I - V characteristics of Ge, Si and GaAs pn Junctions

Fig 6.4

Minority Carrier
Concentration

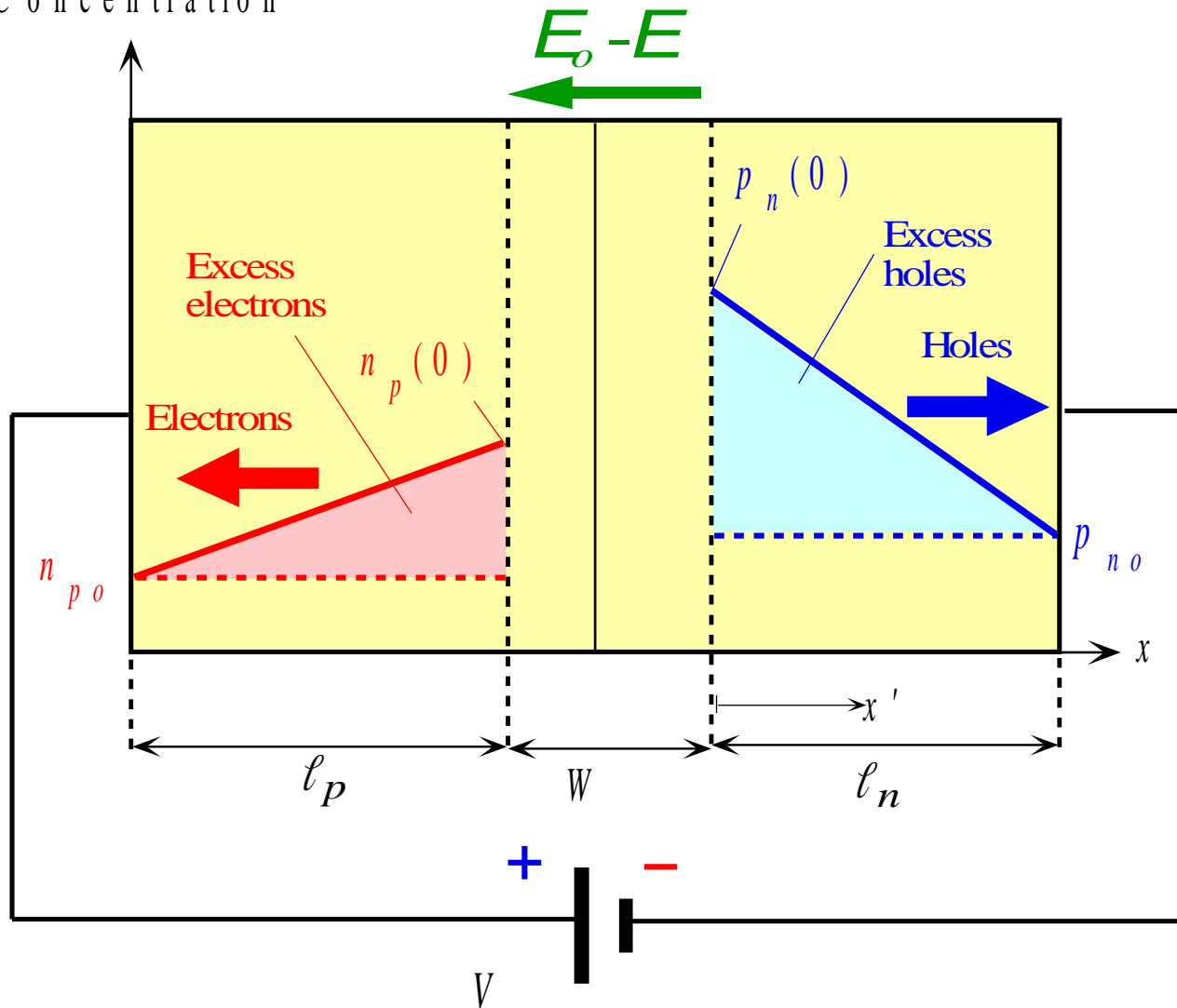


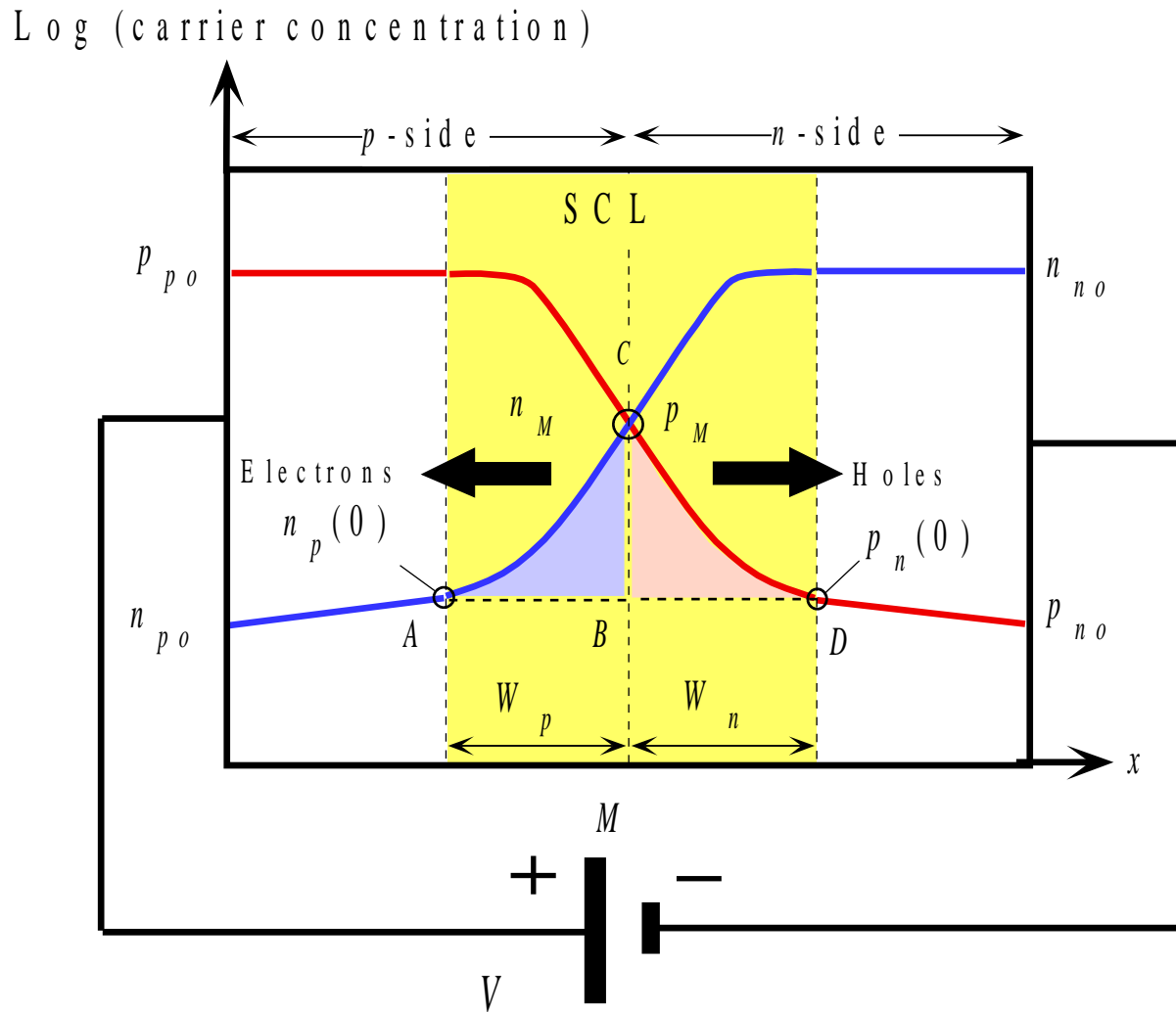
Fig 6.5

Forward Bias: Diffusion Current

Short Diode

$$J = \left(\frac{eD_h}{\ell_n N_d} + \frac{eD_e}{\ell_p N_a} \right) n_i^2 \left[\exp\left(\frac{eV}{kT}\right) - 1 \right]$$

where ℓ_n and ℓ_p represent the lengths of the neutral n - and p -regions outside the depletion region.



Forward biased pn junction and the injection of carriers and their recombination in the SCL

Fig 6.6

Forward Bias: Recombination and Total Current

Recombination Current

$$J_{\text{recom}} = J_{ro} [\exp(eV / 2kT) - 1] \quad \text{where } J_{ro} = \frac{en_i}{2} \left(\frac{W_p}{\tau_e} + \frac{W_n}{\tau_h} \right)$$

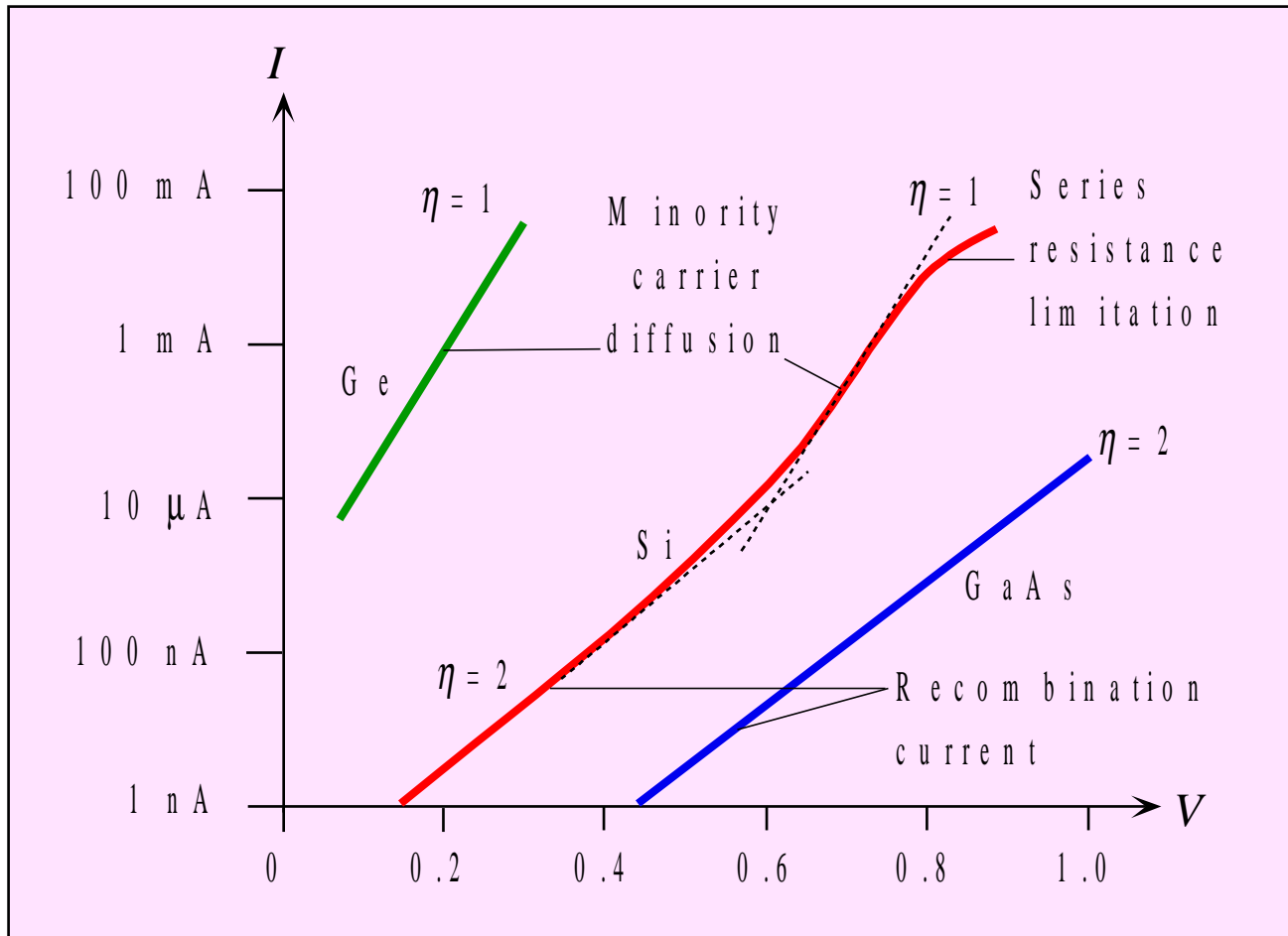
Total diode current = diffusion + recombination

$$J = J_{so} \exp\left(\frac{eV}{kT}\right) + J_{ro} \exp\left(\frac{eV}{2kT}\right) \quad V > \frac{kT}{e}$$

The diode equation

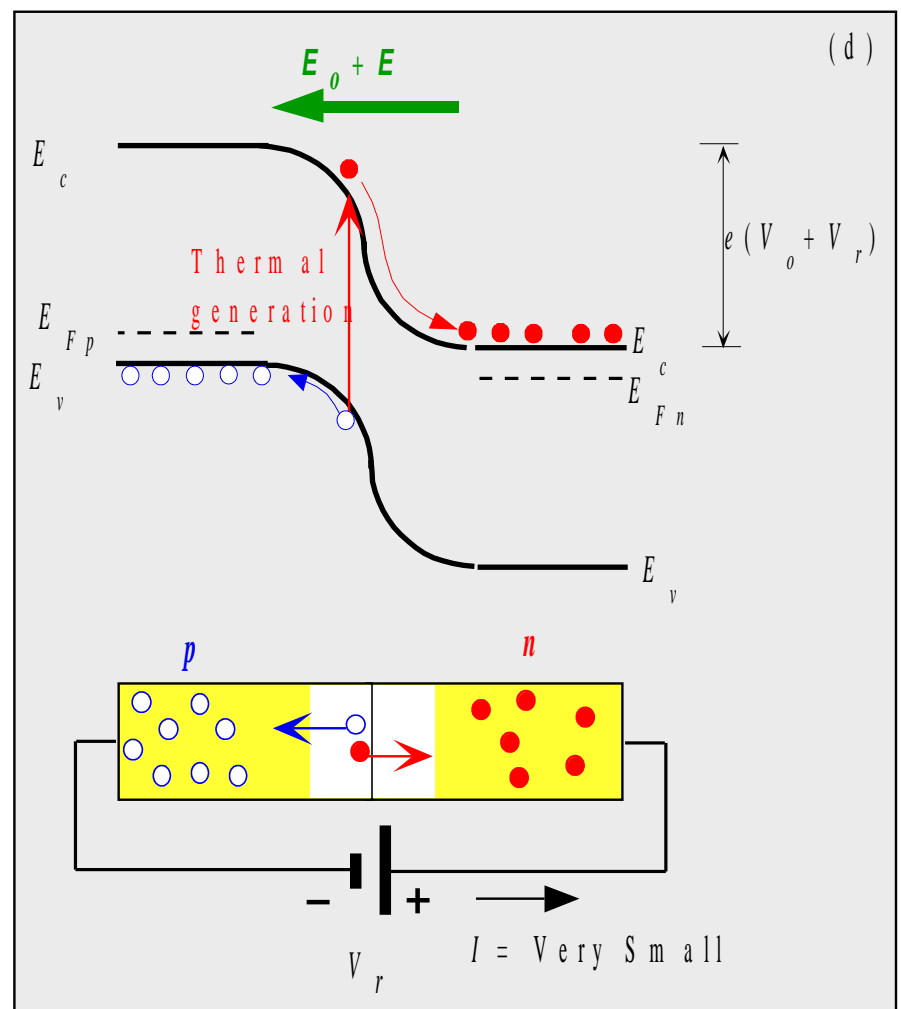
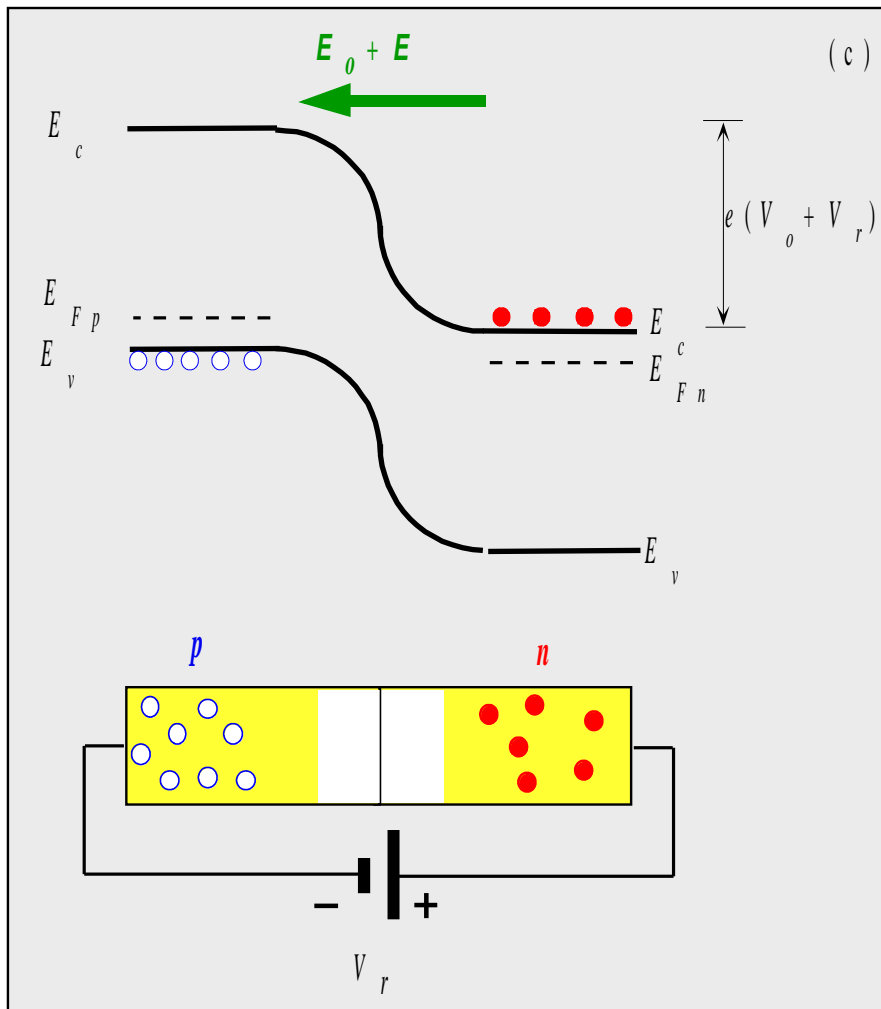
$$J = J_o \exp\left(\frac{eV}{\eta kT}\right) \quad V > \frac{kT}{e}$$

Where J_o is a new constant and η is an ideality factor



Schematic sketch of typical I - V characteristics of Ge, Si and GaAs pn junctions as $\log(I)$ vs V . The slope indicates $e/(\eta kT)$

Fig 6.7



Energy band diagrams for a pn junction under (c) reverse bias conditions. (d) Thermal generation of electron hole pairs in the depletion region results in a small reverse current.

Fig 6.11

Reverse Bias

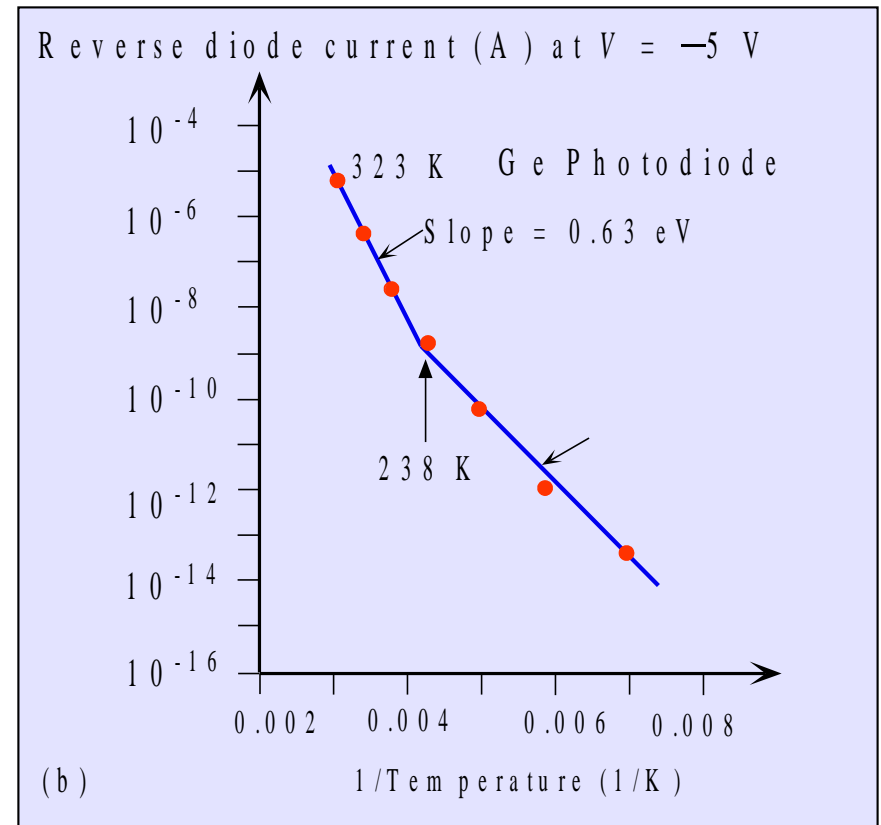
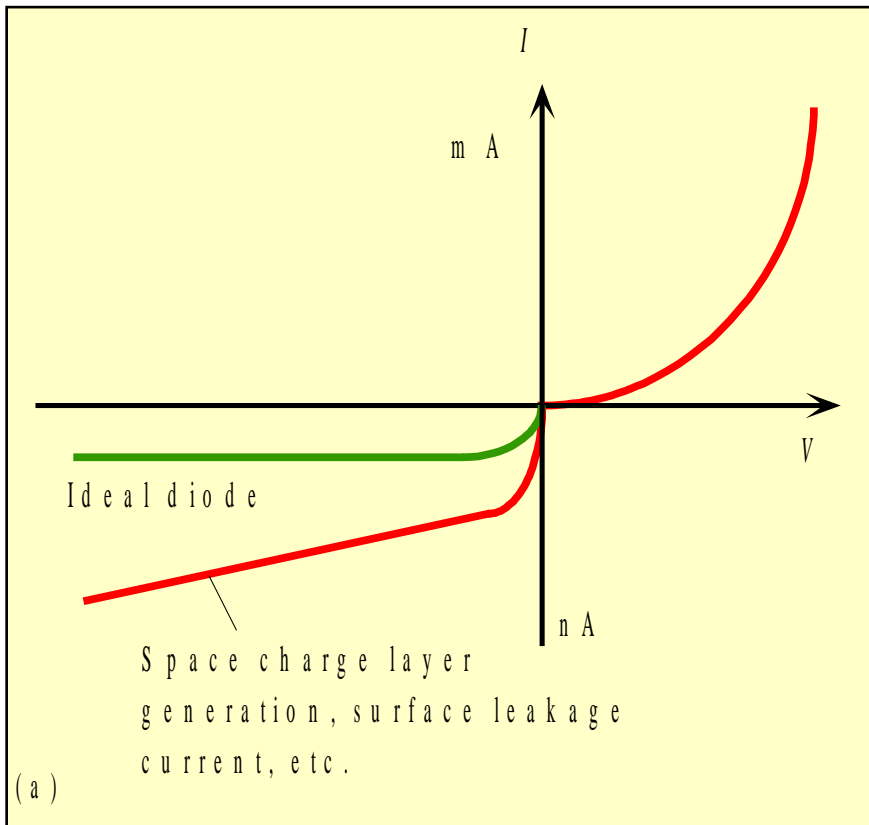
Total Reverse Current

$$J_{\text{rev}} = \left(\frac{eD_h}{L_h N_d} + \frac{eD_e}{L_e N_a} \right) n_i^2 + \frac{eWn_i}{\tau_g}$$

Thermal generation in depletion region

Mean thermal generation time

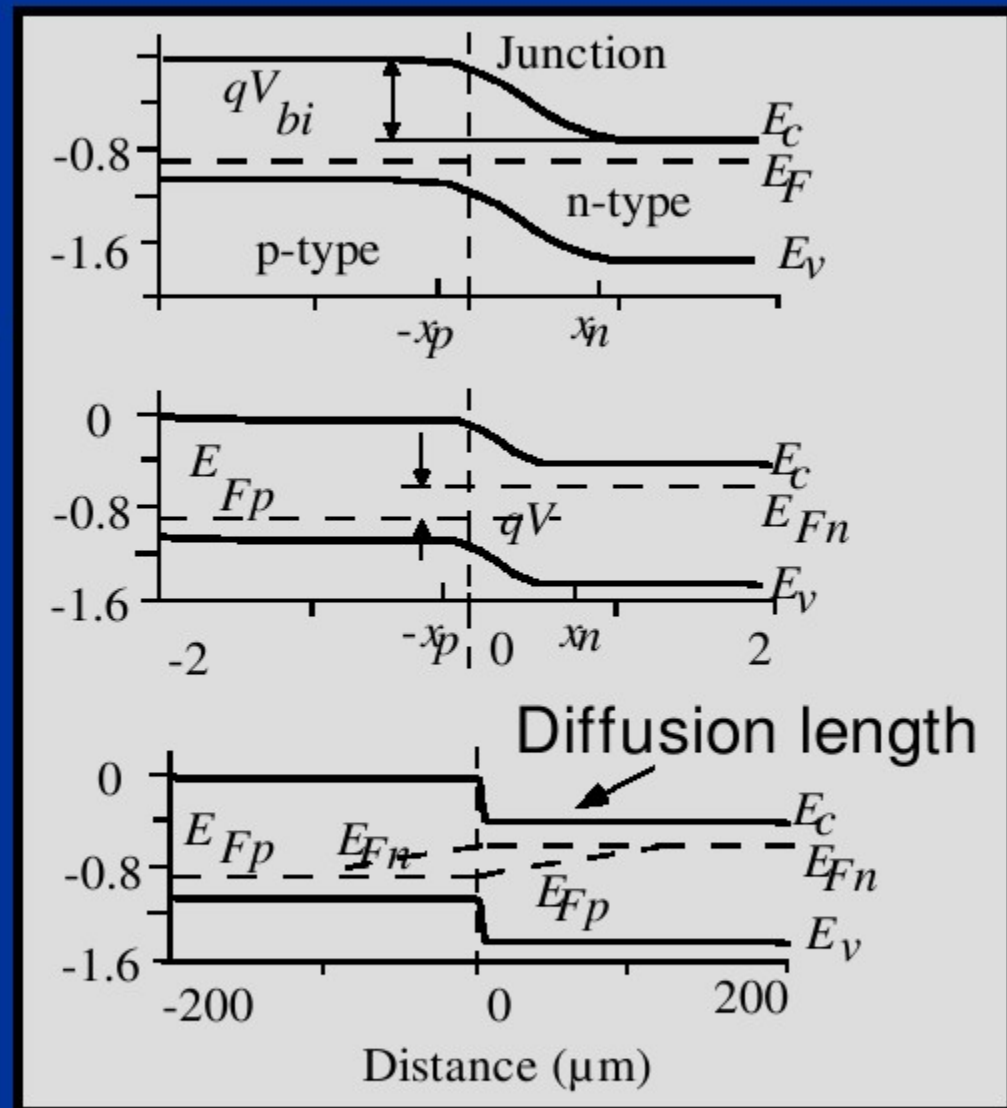
Diffusion current in neutral regions
the Shockley reverse current



(a) Reverse I-V characteristics of a pn junction (the positive and negative current axes have different scales). (b) Reverse diode current in a Ge pn junction as a function of temperature in a $\ln(I_{rev})$ vs $1/T$ plot. Above 238 K, I_{rev} is controlled by n_i^2 and below 238 K it is controlled by n_i . The vertical axis is a logarithmic scale with actual current values. (From D. Scansen and S.O. Kasap, *Cnd. J. Physics*, **70**, 1070-1075, 1992.)

Fig 6.9

Band Diagrams



Law of the Junction

$$qV = E_{Fn} - E_{Fp}$$
$$pn = n_i^2 \exp\left(\frac{E_{Fn} - E_{Fp}}{k_B T}\right) = n_i^2 \exp\left(\frac{V}{V_{th}}\right)$$

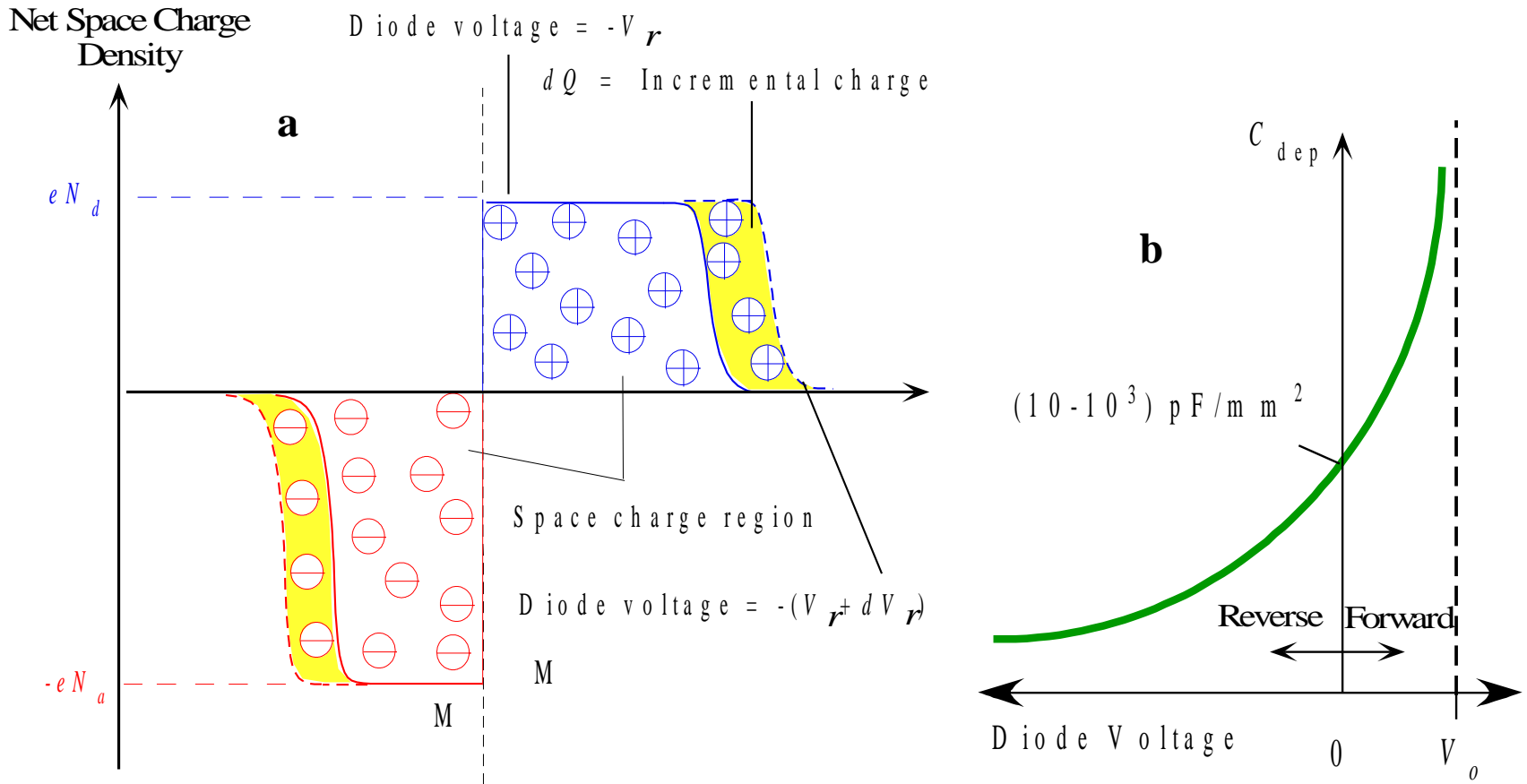
Example

The intrinsic carrier concentration in GaAs at 300 K is approximately 10^6 cm^{-3} . Estimate the forward bias required to create the electron-hole density of 10^{17} cm^{-3} in the depletion region at the point where $p = n$.

Solution

From the law of the junction

$$V = V_{th} \ln \frac{pn}{v_i^2} = 0.02584 \times \ln \frac{10^{34}}{10^{12}} = 1.308 V$$



The depletion region behaves like a capacitor. (a) The charge in the depletion region depends on the applied voltage just as in a capacitor (b) The incremental capacitance of the depletion region increases with forward bias and decreases with reverse bias. Its value is typically in the range of picofarads per mm^2 of device area.

Fig 6.12

Depletion layer capacitance of the pn junction

Depletion region width

$$W = \left[\frac{2\epsilon(N_a + N_d)(V_o - V)}{eN_a N_d} \right]^{1/2}$$

where, for forward bias, V is positive, which reduces V_o , and, for reverse bias, V is negative, so V_o is increased.

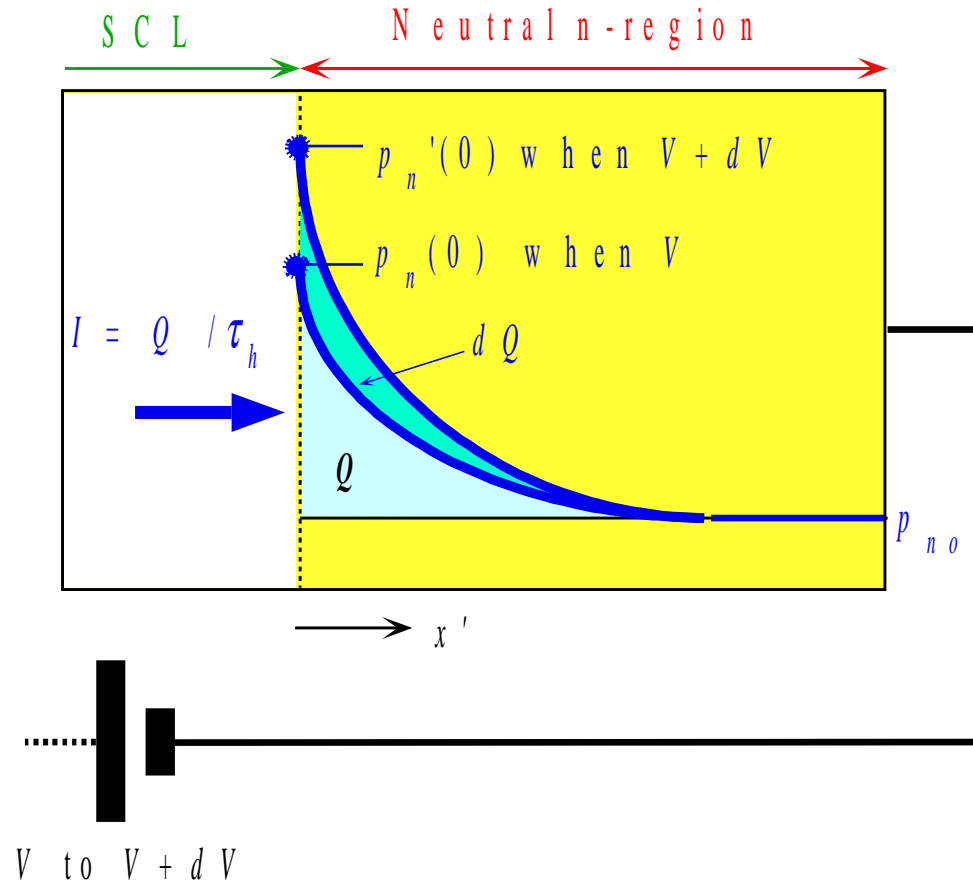
Definition of depletion layer capacitance C_{dep}

$$C_{\text{dep}} = \left| \frac{dQ}{dV} \right|$$

where the amount of charge on any one side of the depletion layer is $|Q| = eN_d W_n A = eN_a W_p A$ and $W = W_n + W_p$

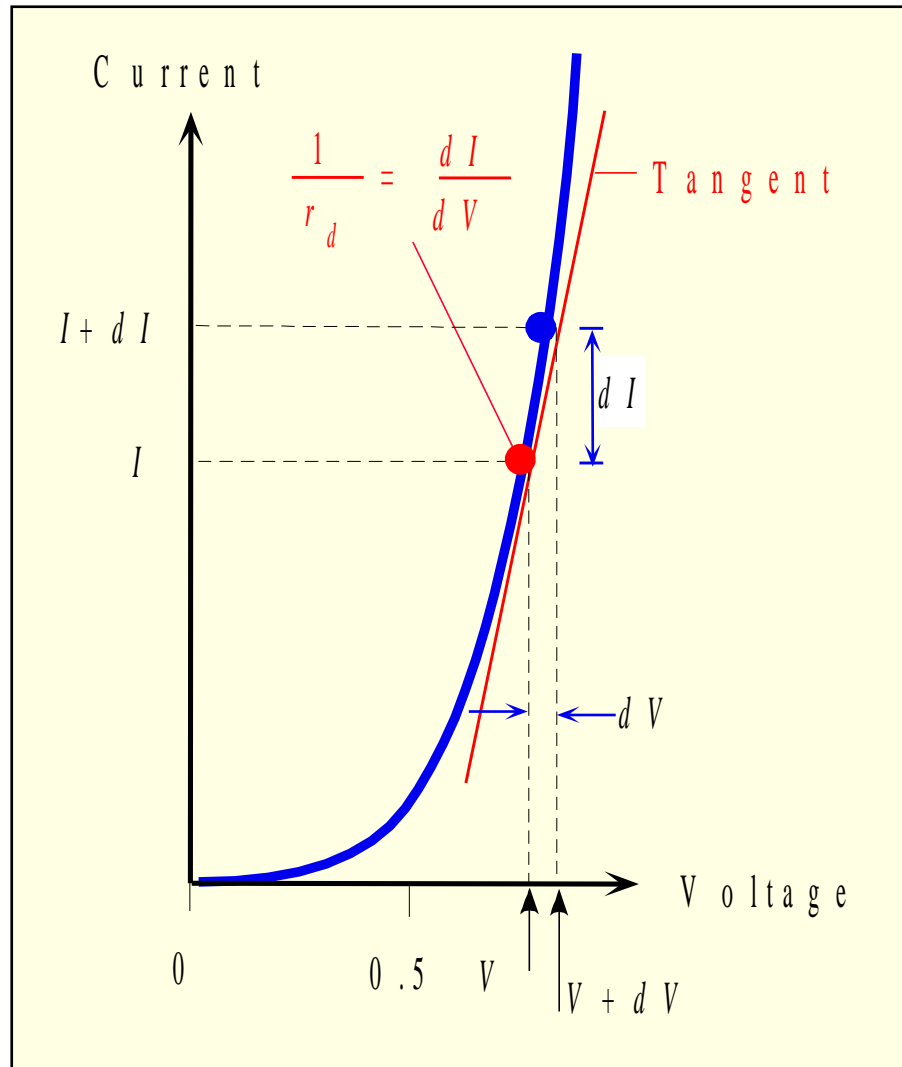
Depletion Capacitance

$$C_{\text{dep}} = \frac{\epsilon A}{W} = \frac{A}{(V_o - V)^{1/2}} \left[\frac{e\epsilon(N_a N_d)}{2(N_a + N_d)} \right]^{1/2}$$



Consider the injection of holes into the n -side during forward bias. Storage or diffusion capacitance arises because when the diode voltage increases from V to $V + dV$ then more minority carriers are injected and more minority carrier charge is stored in the n -region.

Fig 6.13



The dynamic resistance of the diode is defined as dV/dI which is the inverse of the tangent at I .

Fig 6.14

Diffusion capacitance and dynamic resistance

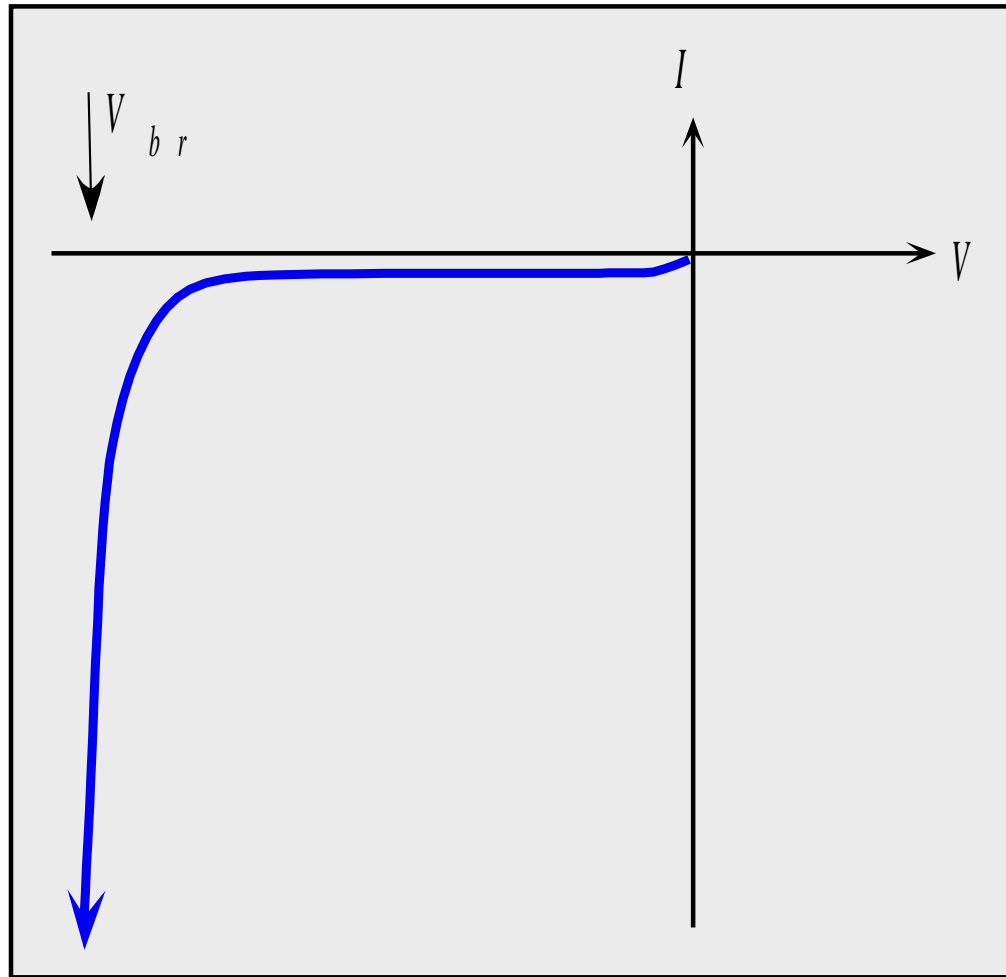
Diffusion capacitance

$$C_{\text{diff}} = \frac{dQ}{dV} = \frac{\tau_h e I}{kT} = \frac{\tau_h I(\text{mA})}{25}$$

where we used $e/kT \approx 40 = 1/0.025$ at room temperature

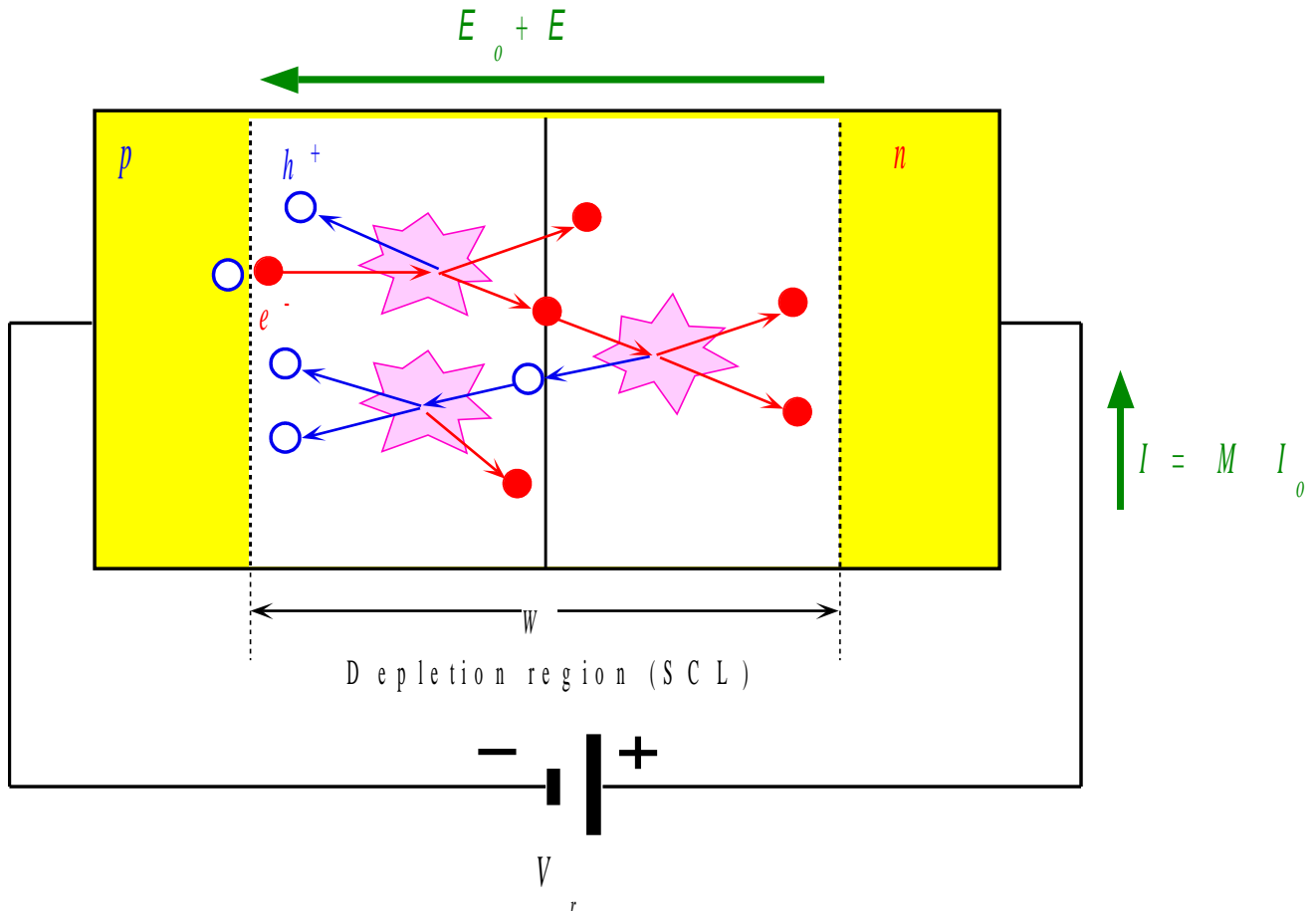
Dynamic incremental resistance

$$r_d = \frac{dV}{dI} = \frac{kT}{eI} = \frac{25}{I(\text{mA})}$$



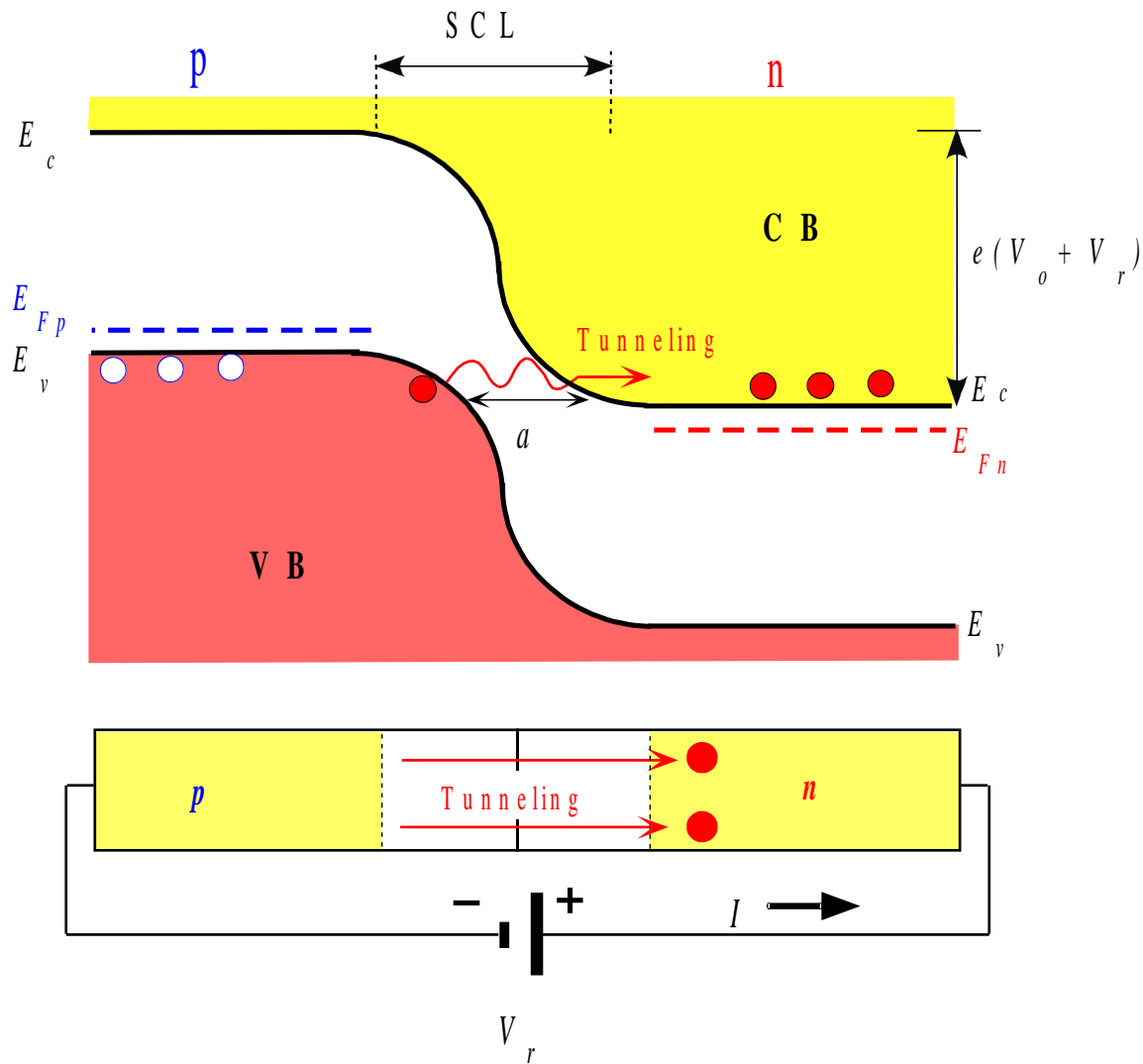
Reverse I - V characteristics of a pn junction.

Fig 6.15



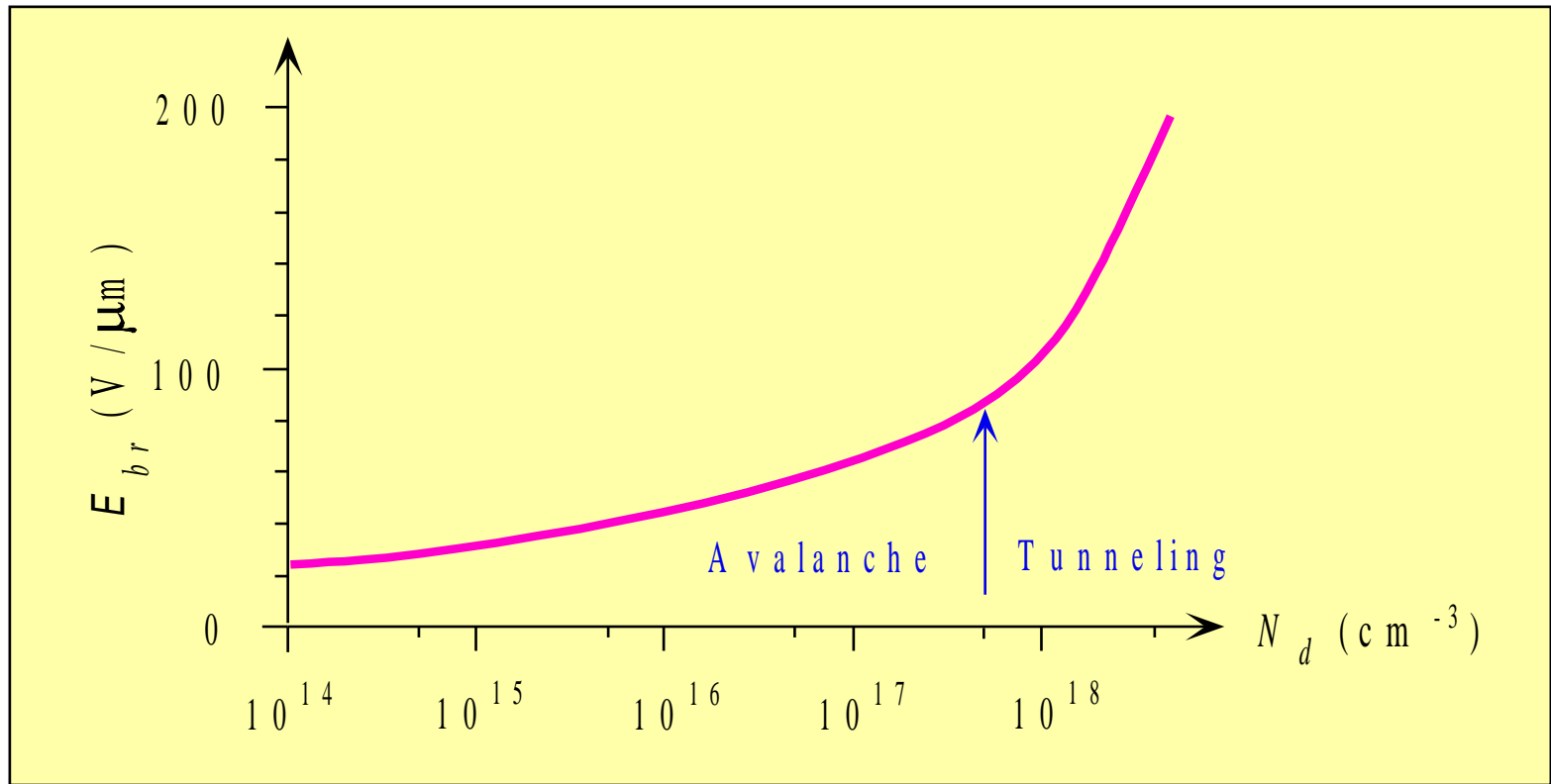
Avalanche breakdown by impact ionization.

Fig 6.16



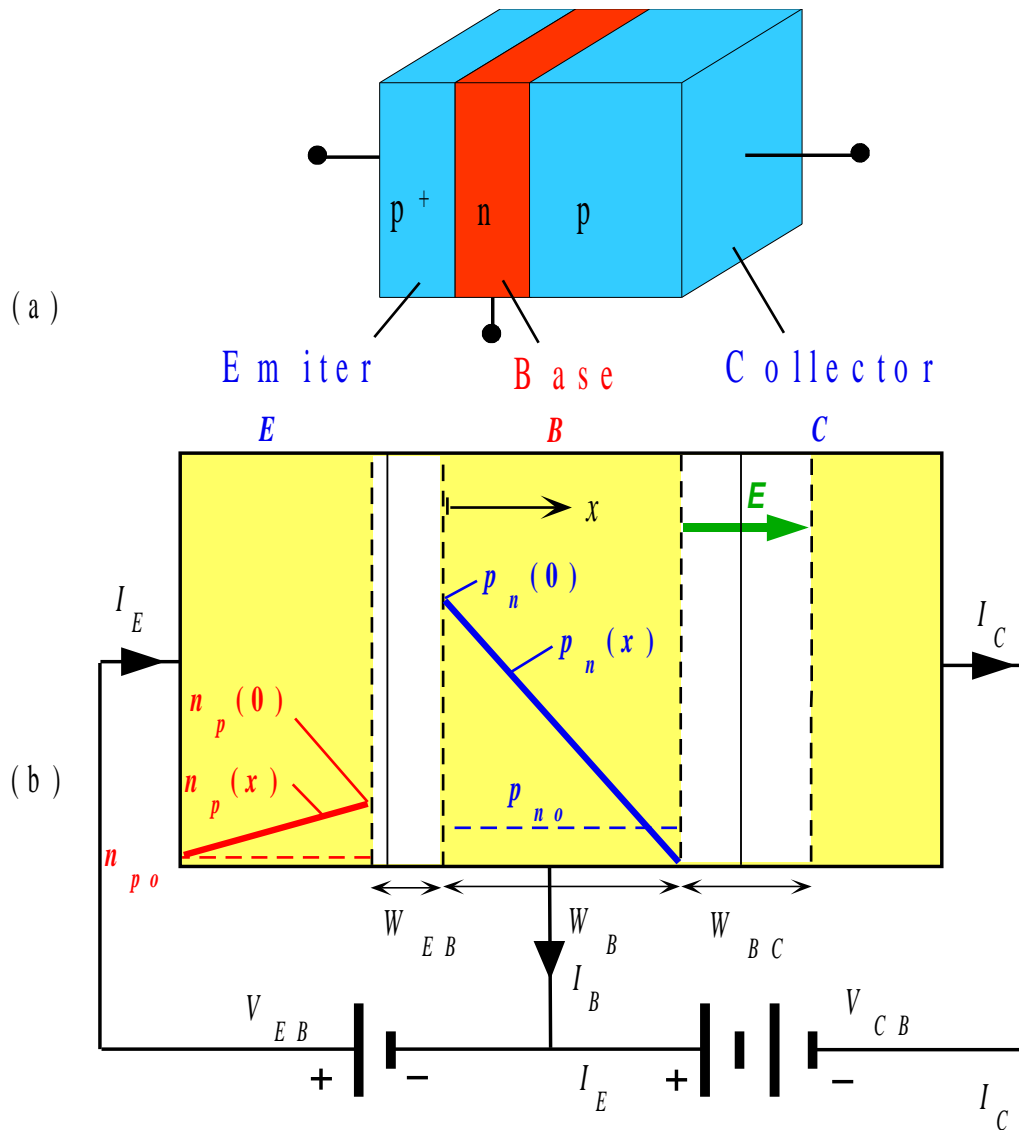
Zener breakdown involves electrons tunneling from the VB of p side to the CB of n -side when the reverse bias reduces E_c to line up with E_v .

Fig 6.18



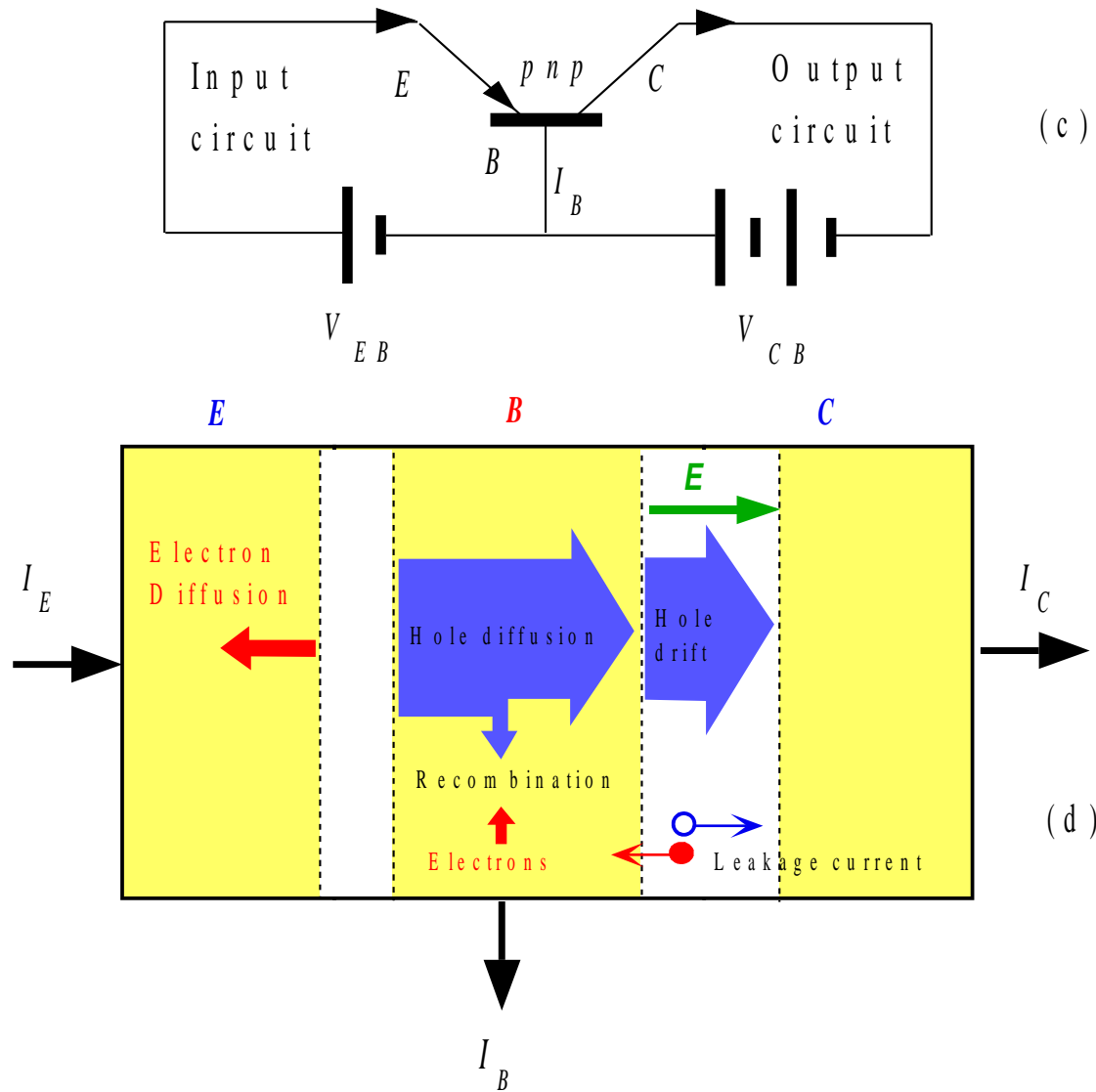
The breakdown field E_{br} in the depletion layer for the onset of reverse breakdown vs. doping concentration N_d in the lightly doped region in a one-sided (p^+n or pn^+) abrupt pn junction. Avalanche and tunneling mechanisms are separated by the arrow [data extracted from M. Sze and G. Gibbons, *Solid. State. Electronics*, 9, 831 (1966)]

Fig 6.19



(a) A schematic illustration of the pnp bipolar transistor with three differently doped regions. (b) The pnp bipolar operated under normal and active conditions.

Fig 6.20



(c) The CB configuration with input and output circuits identified. (d) The illustration of various current components under normal and active conditions.

Fig 6.20

Emitter Junction: The Law of the Junction

Hole concentration just outside the depletion region in the base at the emitter end

$$p_n(0) = p_{no} \exp\left(\frac{eV_{EB}}{kT}\right)$$

where V_{EB} is the forward bias applied across the emitter-base (EB) junction

Hole concentration just outside the depletion region in the base at the collector end

$$p_n(W_B) \approx 0$$

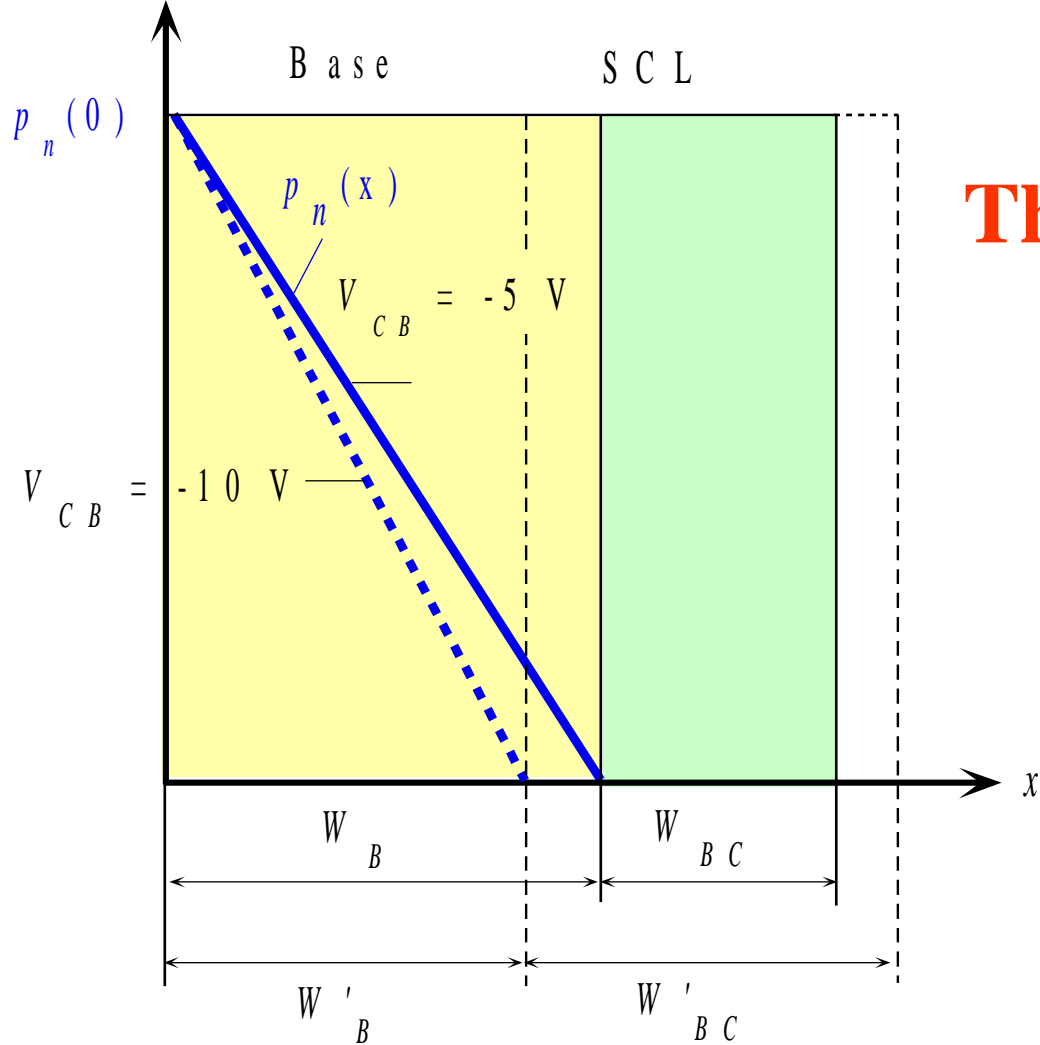
The Emitter Current

Holes diffuse through the base, from the emitter end to the collector end. This diffusion is driven by the hole concentration gradient dp_n/dx .

Assume that the hole concentration profile is linear; it decreases from $p_n(0)$ to 0 over the neutral base width W_B . (Initially, neglect the recombination of holes with electrons

in the base.)

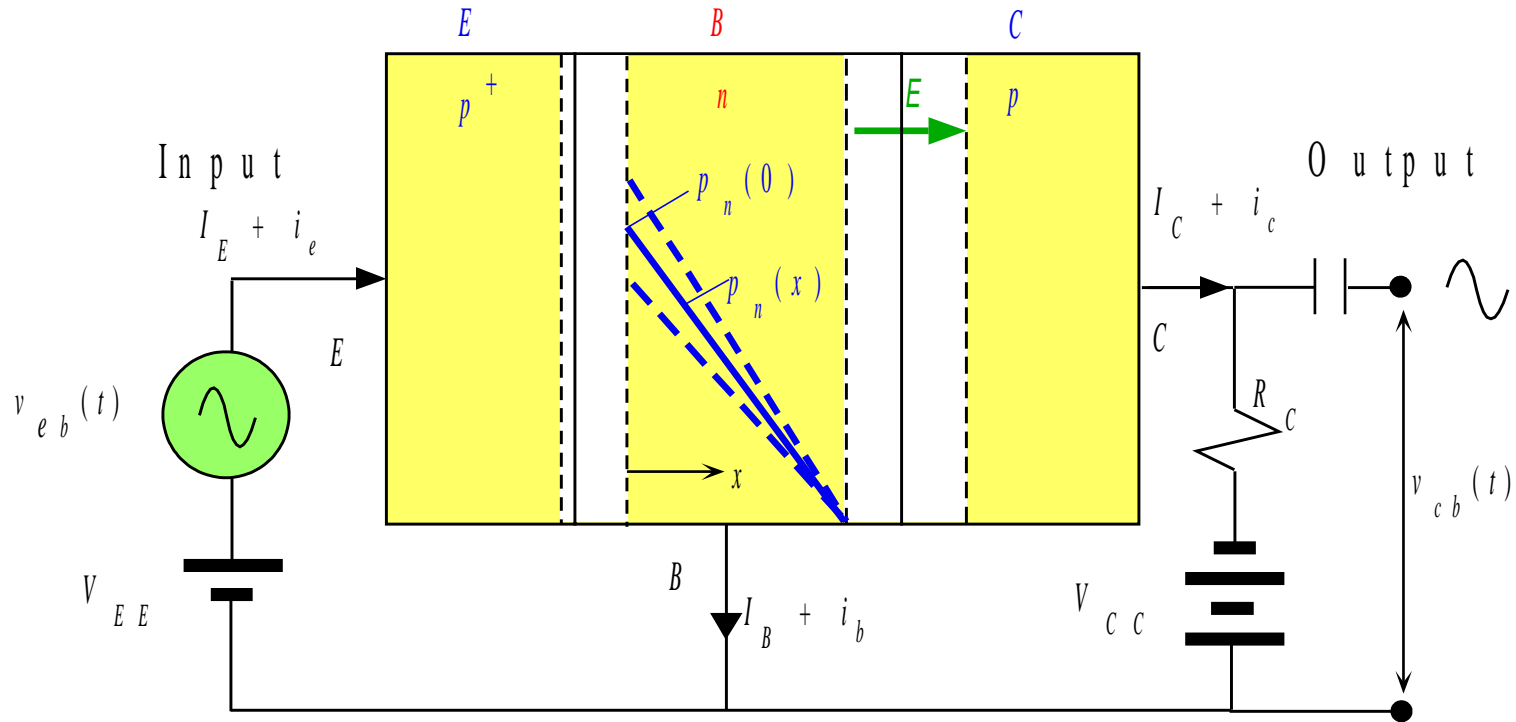
$$I_E = -eAD_h \left(\frac{dp_n}{dx} \right)_{x=0} = \frac{eAD_h p_n(0)}{W_B}$$



The Early Effect

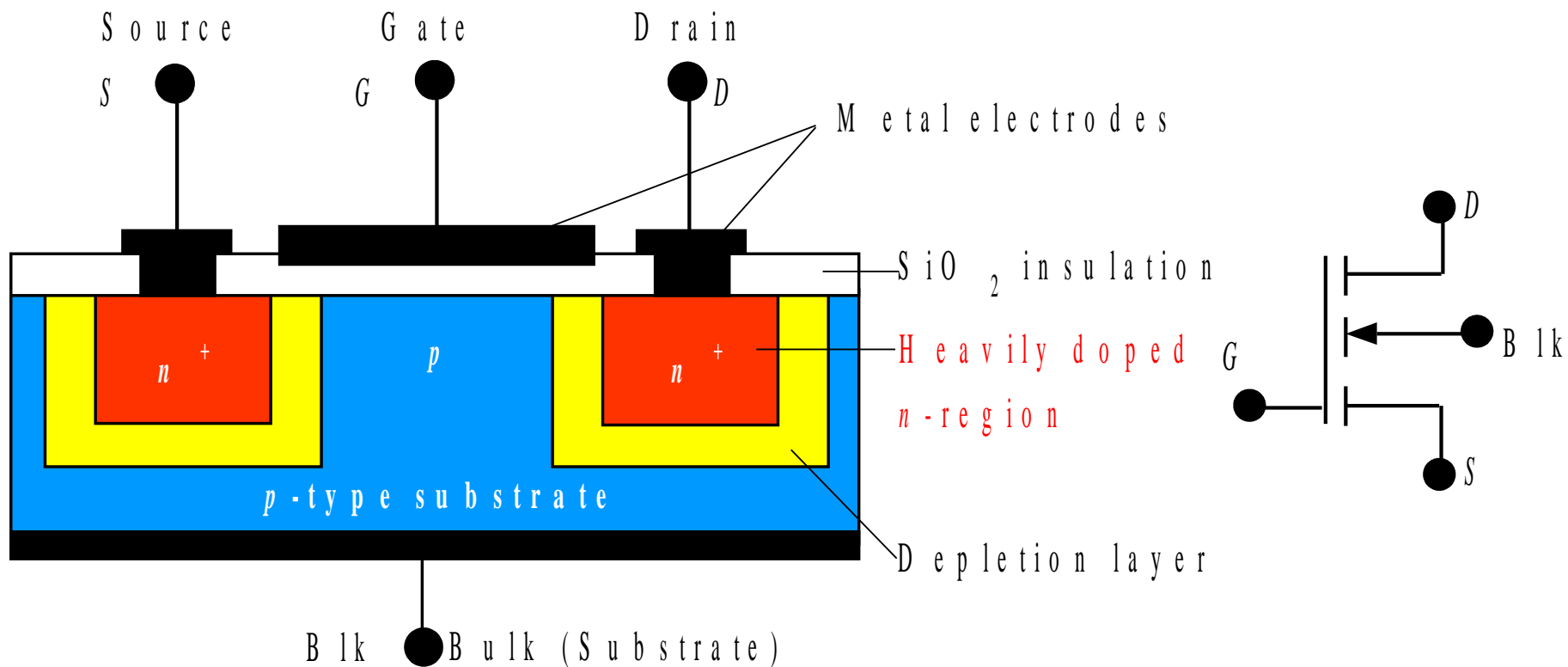
The Early effect. When the BC reverse bias increases, the depletion width W_{BC} increases to W'_{BC} which reduces the base width W_B to W'_B . As $p_n(0)$ is constant (constant V_{EB}), the minority carrier concentration gradient becomes steeper and the collector current I_C increases.

Fig 6.22



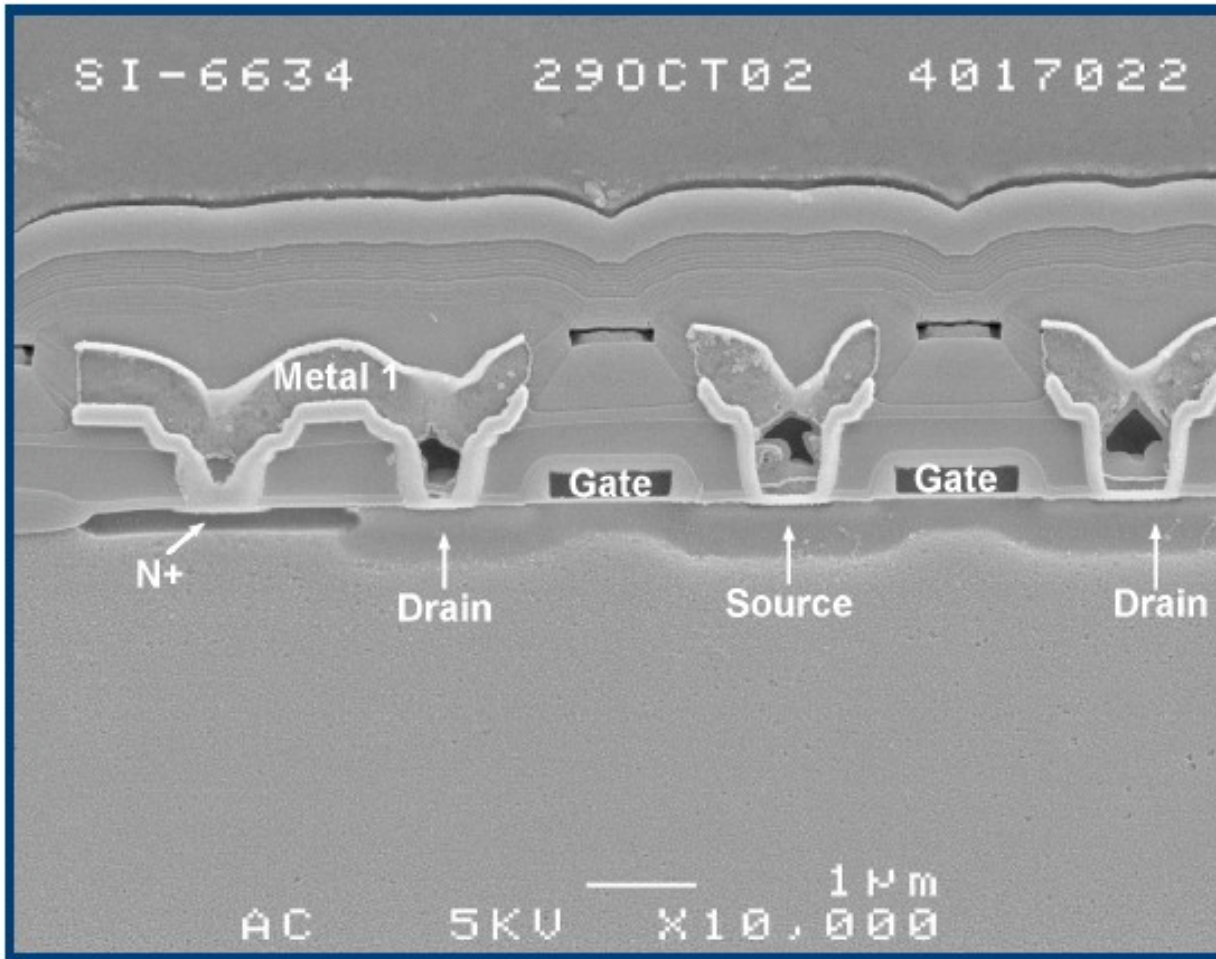
A pnp transistor operated in the active region in the common base amplifier configuration. The applied (input) signal v_{eb} modulates the dc voltage across the BE junction and hence modulates the injected hole concentration up and down about the dc value $p_n(0)$. The solid line shows $p_n(x)$ when only the dc bias V_{EE} is present. The dashed lines show how $p_n(x)$ is modulated up and down by the signal v_{eb} superimposed on V_{EE} .

Fig 6.23



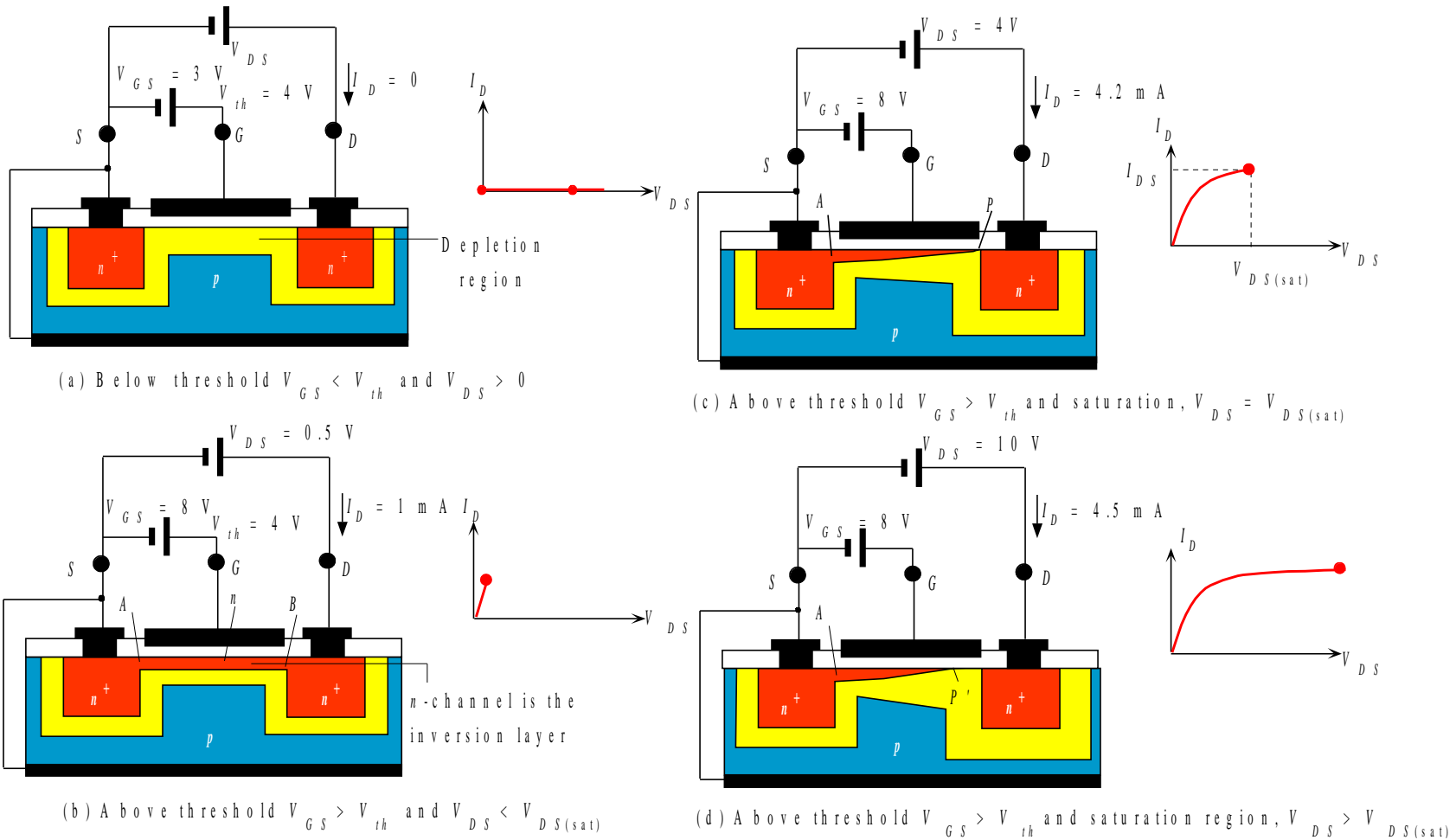
The basic structure of the enhancement MOSFET and its circuit symbol.

Fig 6.36



SEM cross section of a MOS Transistor

[SOURCE: Courtesy of Don Scansen, Semiconductor Insights, Kanata, Ontario, Canada

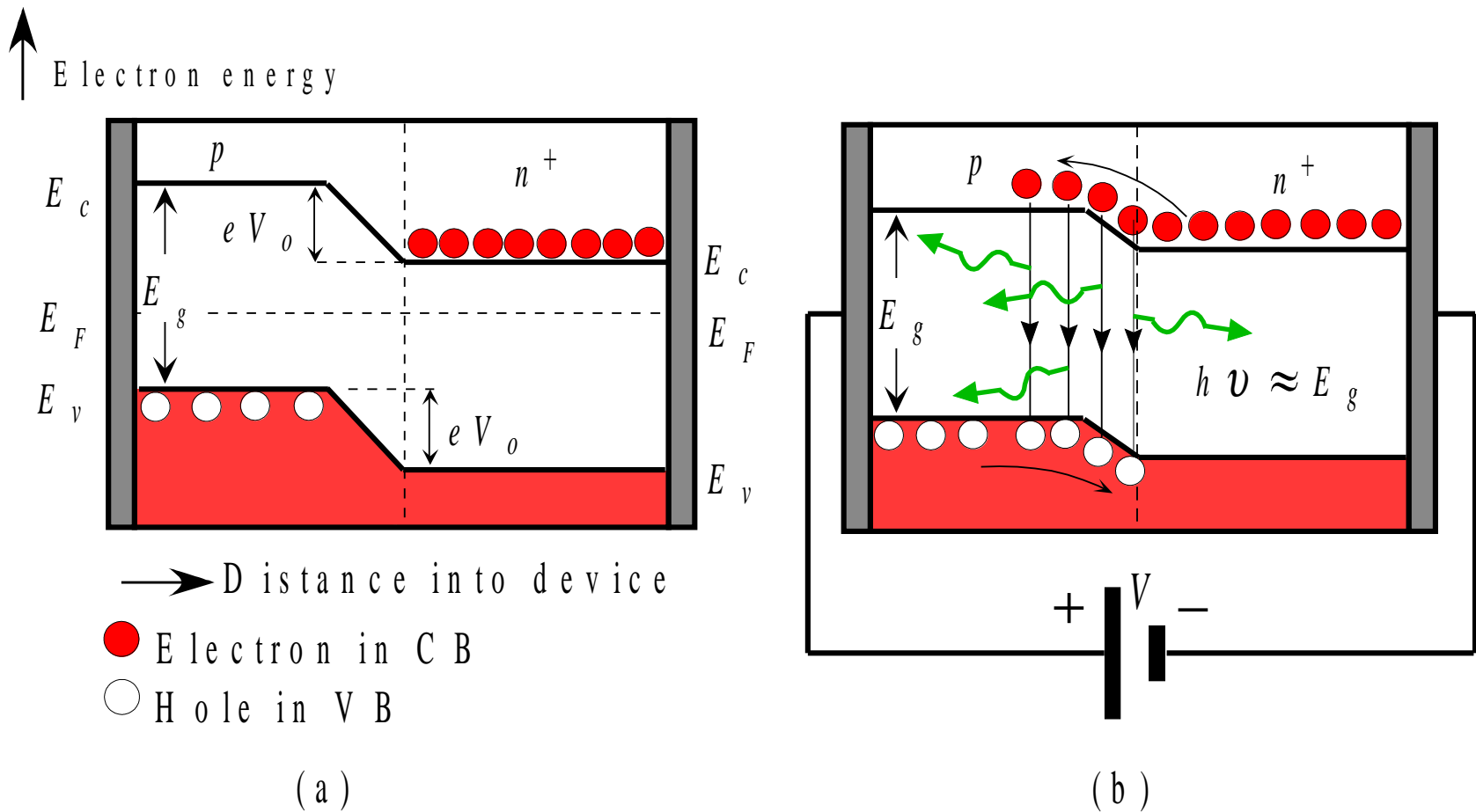


The MOSFET I_D vs V_{DS} characteristics

Fig 6.37

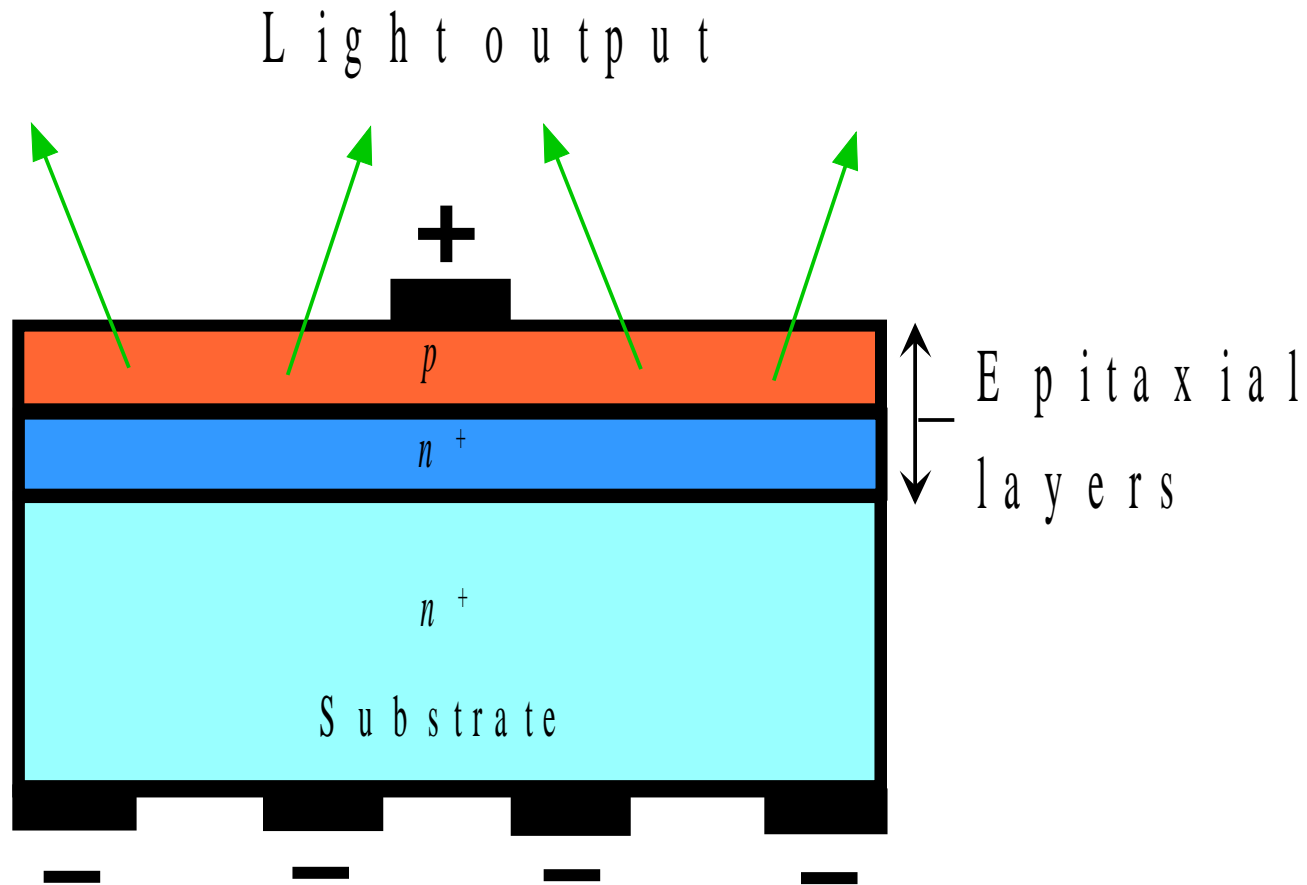
Optical Devices

- LED – pn diodes in a direct band-gap semiconductor
 - Doping with traps for indirect semiconductors
 - Hetro-junctions
 - Spectrum
- Solar Cells
 - Photo-currents
 - Materials, Technologies
 - Improvements
- Photodiodes
 - Speed versus sensitivity



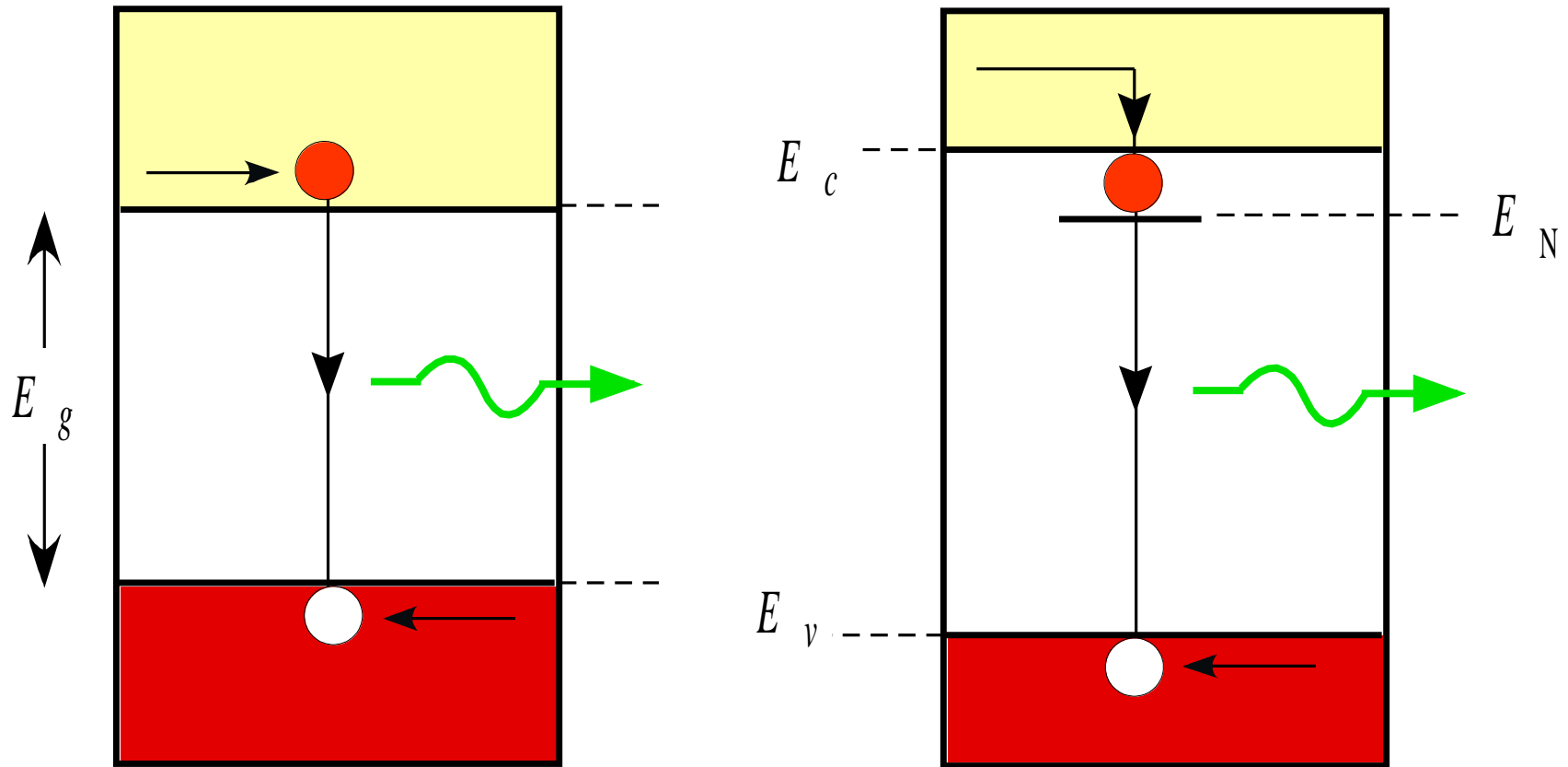
(a) The energy band diagram of a p - n^+ (heavily n -type doped) junction without any bias. Built-in potential V_o prevents electrons from diffusing from n^+ to p side. (b) The applied bias reduces V_o and thereby allows electrons to diffuse, be injected, into the p -side. Recombination around the junction and within the diffusion length of the electrons in the p -side leads to photon emission.

Fig 6.43



A schematic illustration of one possible LED device structure. First n^+ is epitaxially grown on a substrate. A thin p layer is then epitaxially grown on the first layer.

Fig 6.44



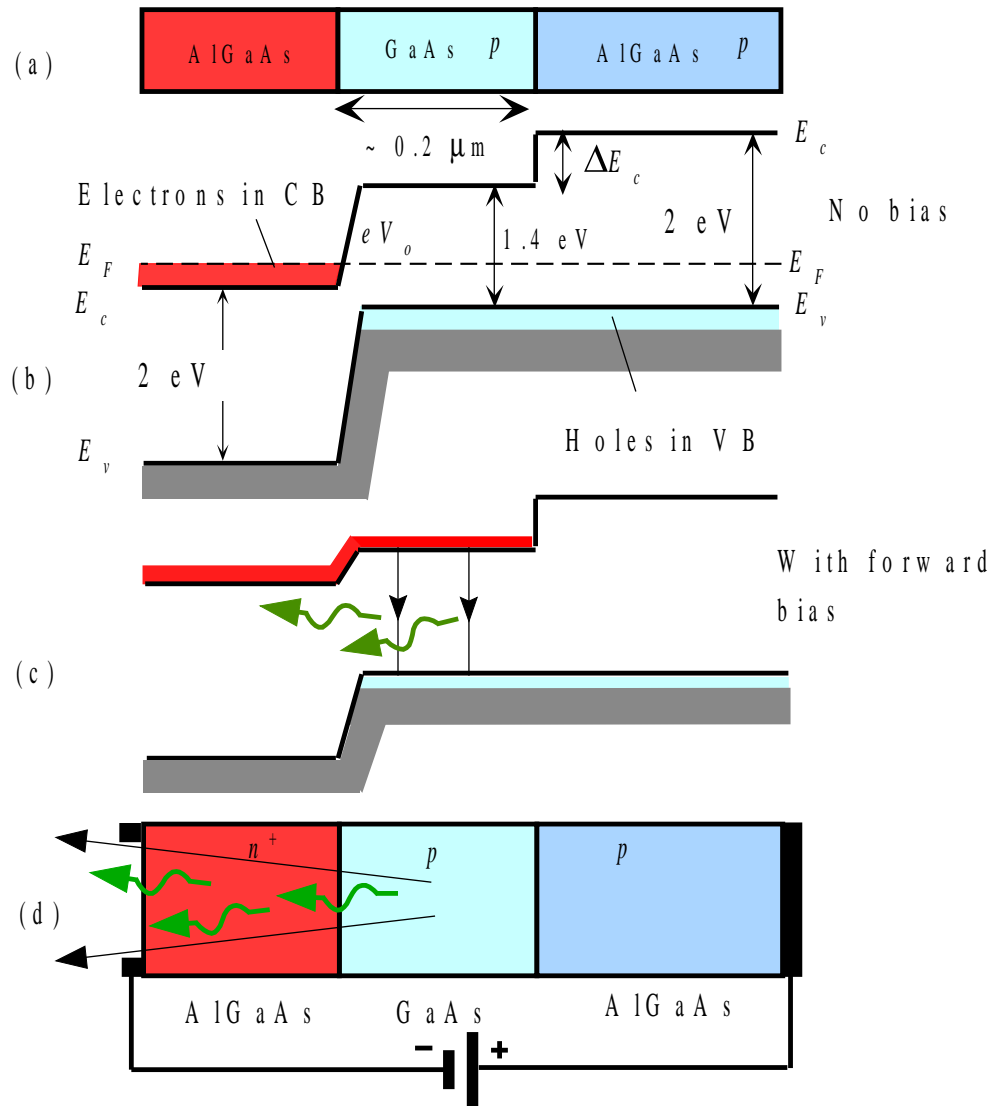
(a) Photon emission in a direct bandgap semiconductor. (b) GaP is an indirect bandgap semiconductor. When doped with nitrogen there is an electron recombination center at E_N . Direct recombination between a captured electron at E_N and a hole emits a photon.

Fig 6.45

Light Emitting Diodes (LED's)

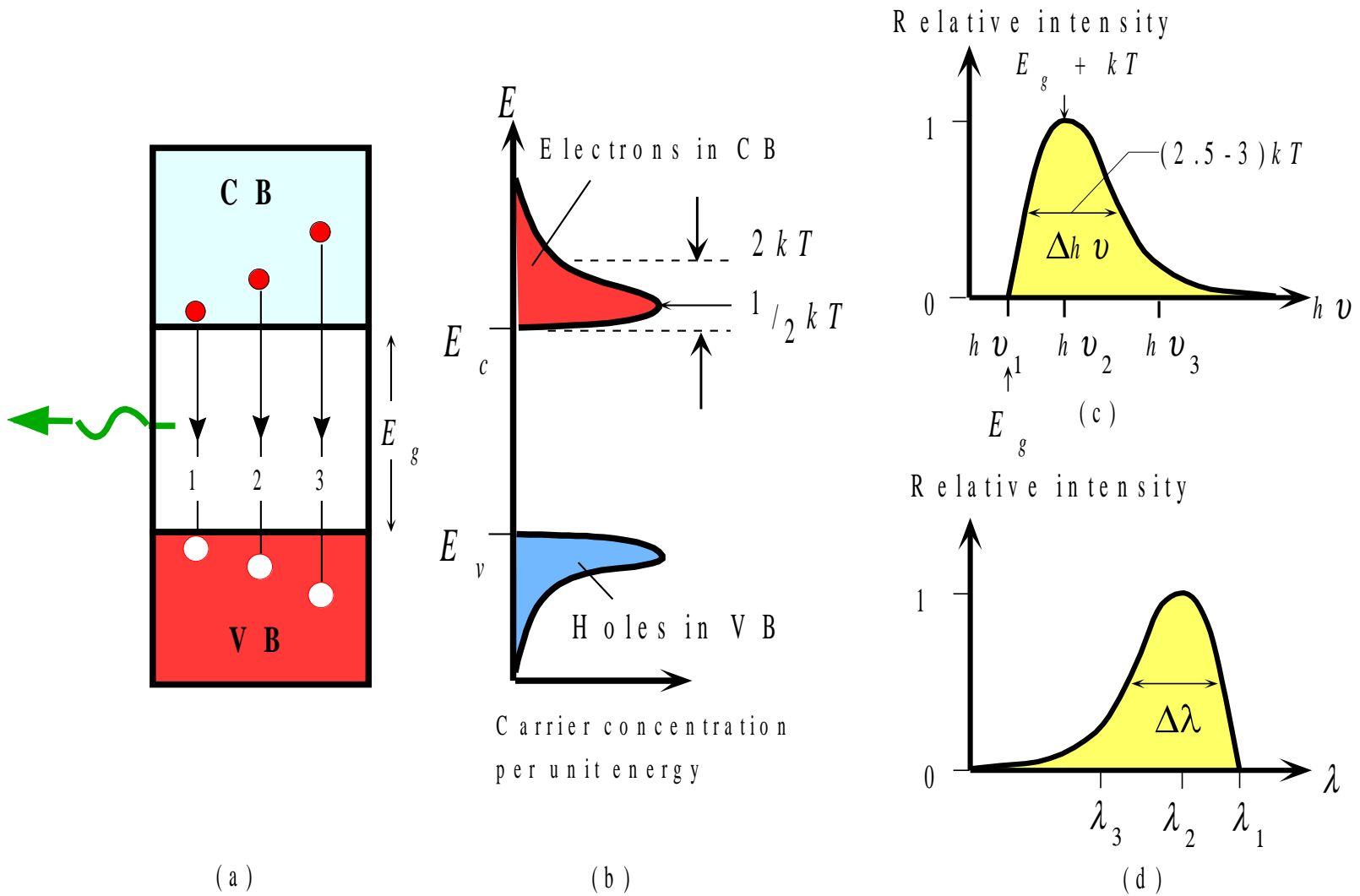
External efficiency, η_{external}

$$\eta_{\text{external}} = \frac{P_{\text{out}} \text{ (optical)}}{IV} \times 100\%$$



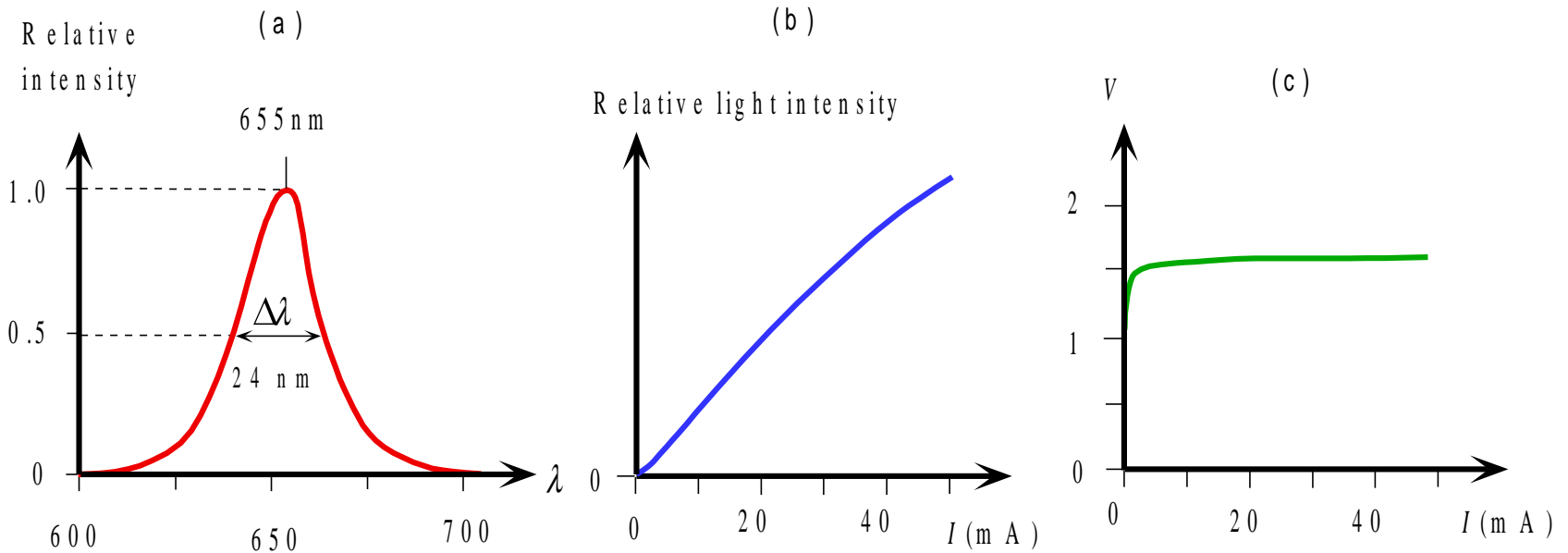
(a) A double heterostructure diode has two junctions which are between two different bandgap semiconductors (GaAs and AlGaAs). (b) A simplified energy band diagram with exaggerated features. E_F must be uniform. (c) Forward biased simplified energy band diagram. (d) Forward biased LED. Schematic illustration of photons escaping reabsorption in the AlGaAs layer and being emitted from the device.

Fig 6.46



(a) Energy band diagram with possible recombination paths. (b) Energy distribution of electrons in the CB and holes in the VB. The highest electron concentration is $(1/2)kT$ above E_c . (c) The relative light intensity as a function of photon energy based on (b). (d) Relative intensity as a function of wavelength in the output spectrum based on (b) and (c).

Fig 6.47



(a) A typical output spectrum (relative intensity vs wavelength) from a red GaAsP LED. (b) Typical output light power vs. forward current. (c) Typical I-V characteristics of a red LED. The turn-on voltage is around 1.5V

Fig 6.48

LED Characteristics

Spread in the emitted photon energies, $\Delta(h\nu)$, is

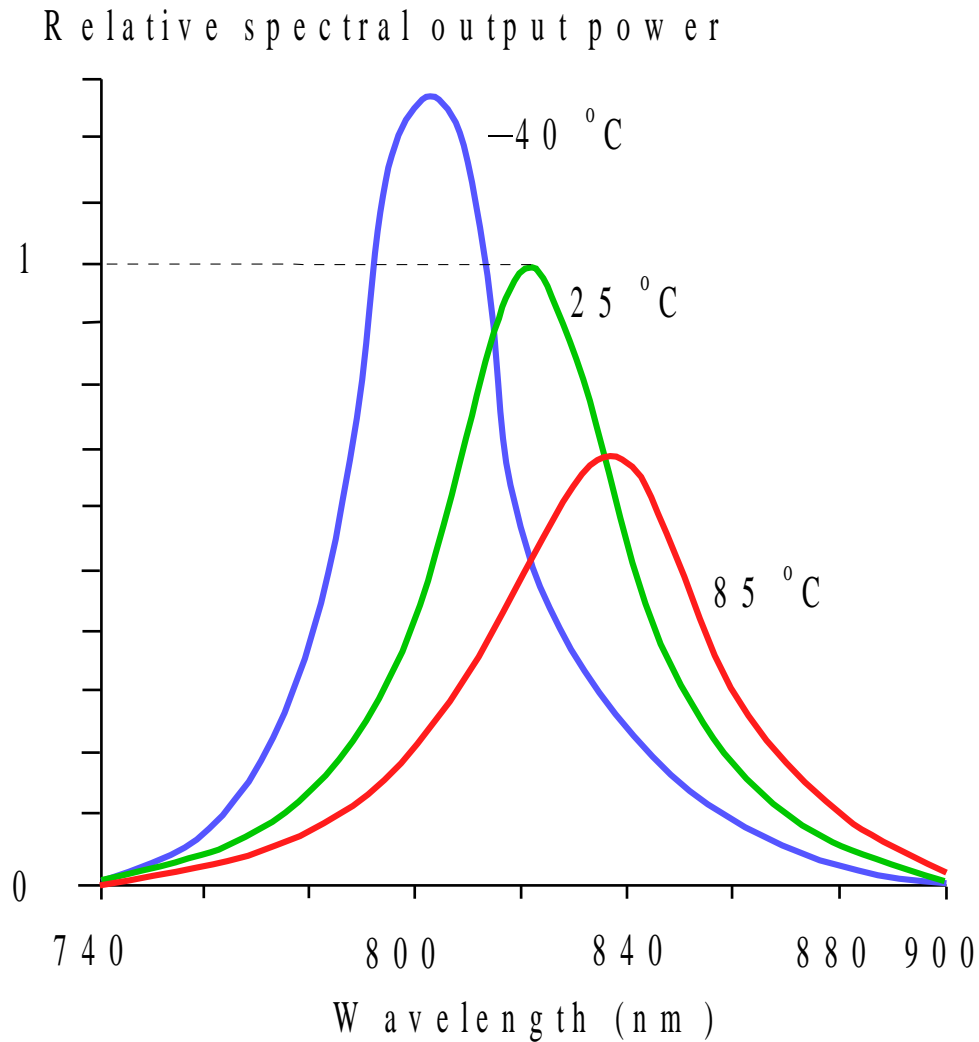
$$\Delta(h\nu) \approx 3kT$$

LED spectral linewidth, $\Delta\lambda$

$$\Delta\lambda = \lambda^2 \frac{3kT}{hc}$$

Example: At room temperature

$$\lambda = 1550 \text{ nm} \rightarrow \Delta\lambda = 150 \text{ nm}$$



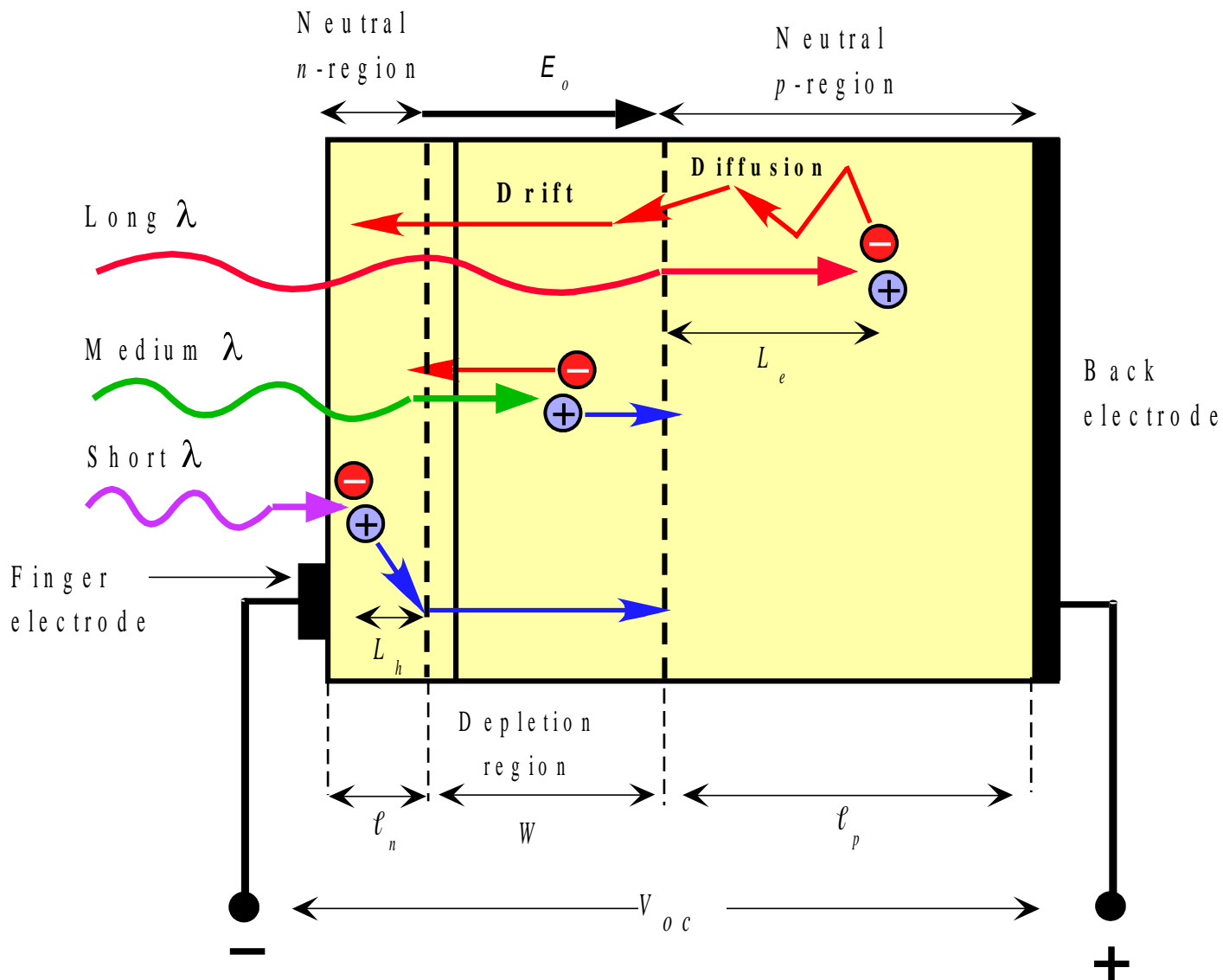
The output spectrum from AlGaAs LED. Values normalized to peak emission at 25 °C

Fig 6.68

Solar Cells

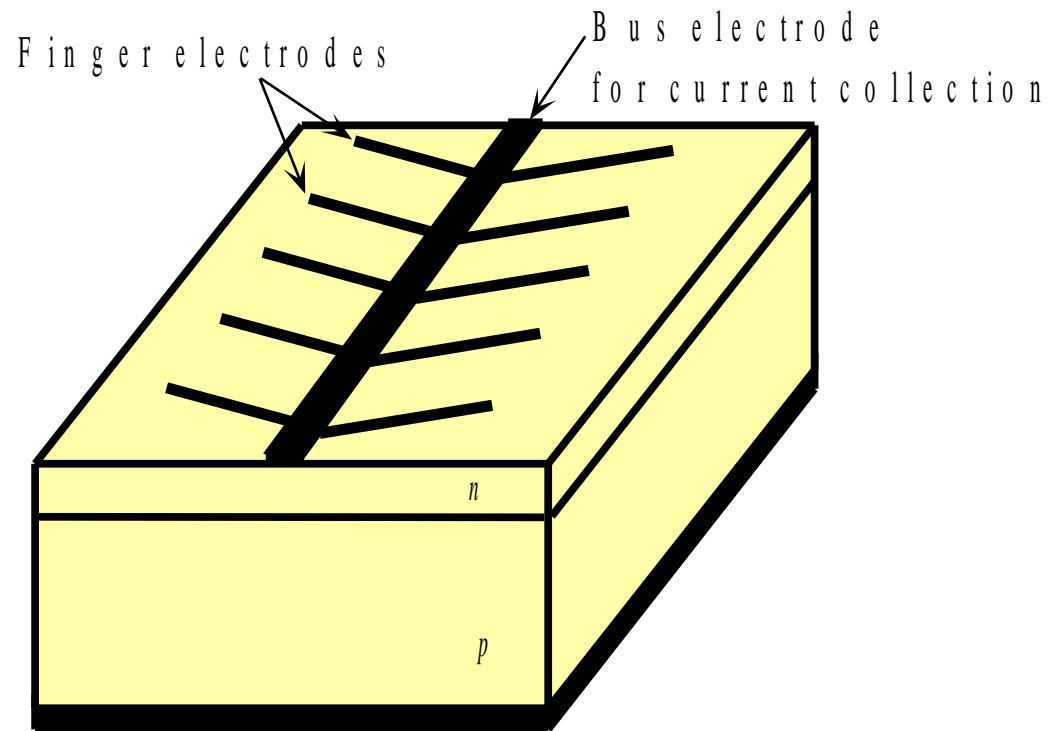
- Hole electron pair generation
- Separation by built in field
- Collection from region (diffusion + W)
- Operation is fwd bias + photon current
- Load line
- Efficiency (FF factor, shunt/series resistance)

Fig 6.68



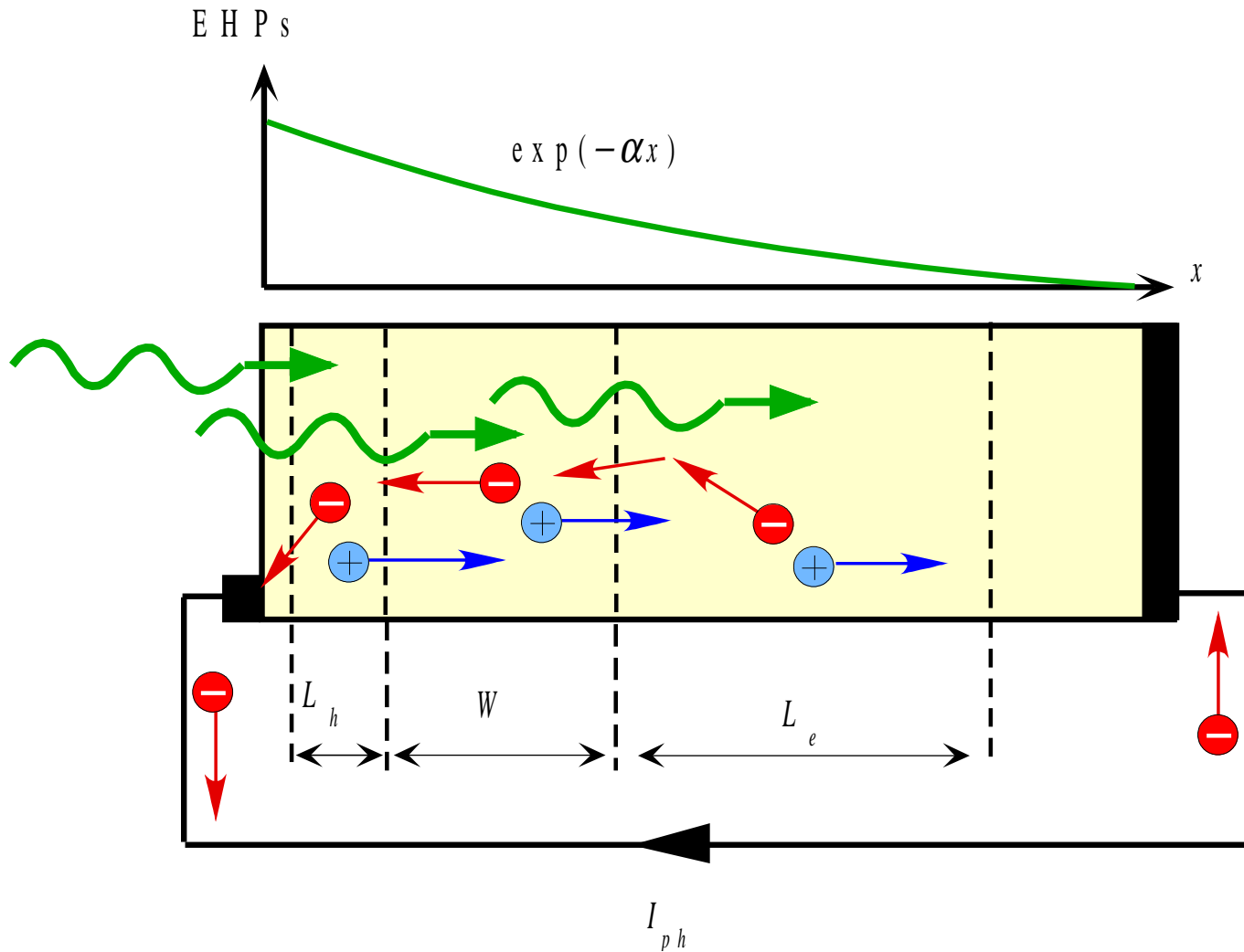
The principle of operation of the solar cell (exaggerated features to highlight principles)

Fig 6.49



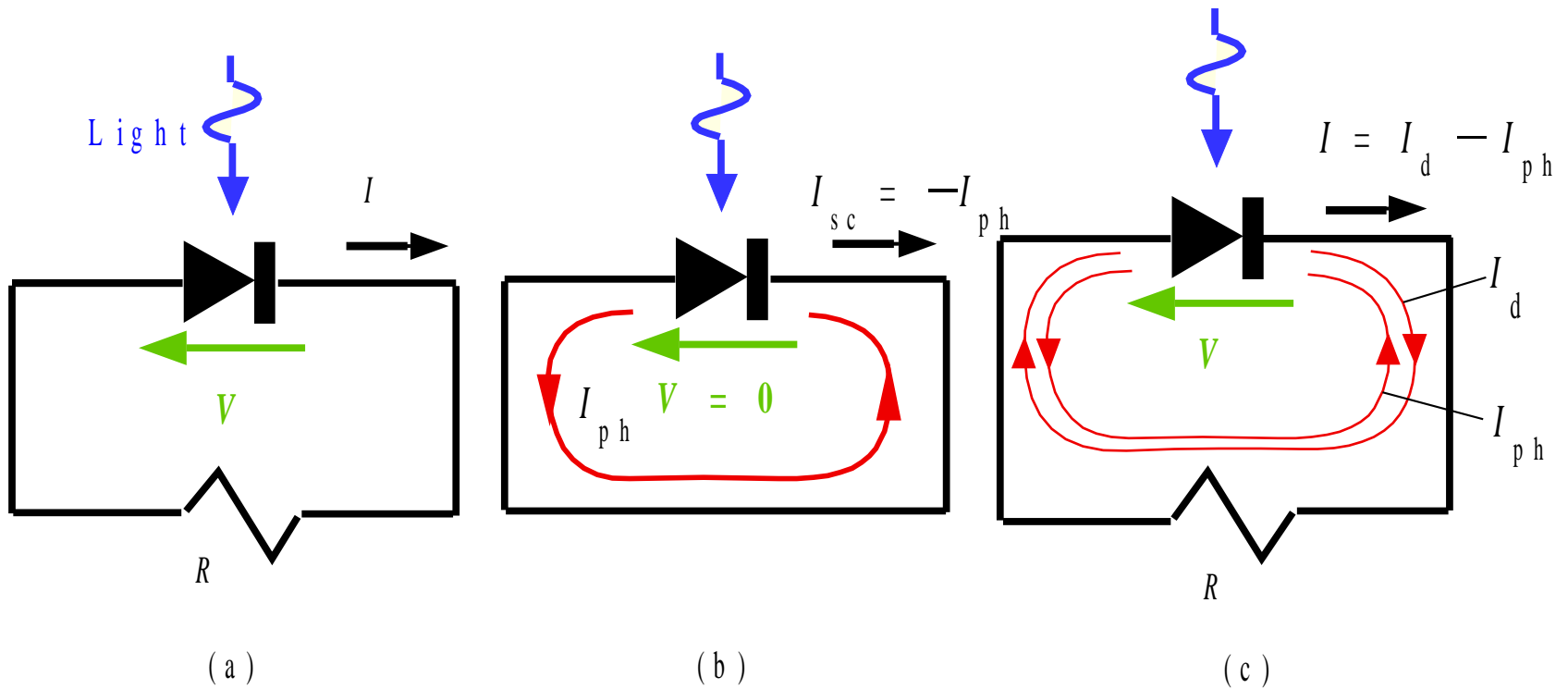
Finger electrodes on the surface of a solar cell reduce the series resistance

Fig 6.50



Photogenerated carriers within the volume $L_h + W + L_e$ give rise to a photocurrent I_{ph} . The variation in the photogenerated EHP concentration with distance is also shown where α is the absorption coefficient at the wavelength of interest.

Fig 6.51



(a) The solar cell connected to an external load R and the convention for the definitions of positive voltage and positive current. (b) The solar cell in short circuit. The current is the photocurrent, I_{ph} . (c) The solar cell driving an external load R . There is a voltage V and current I in the circuit.

Fig 6.52

Solar Cells

Short circuit solar cell current in light

$$I_{sc} = -I_{ph} = -KI$$

↑
Photocurrent generated by light

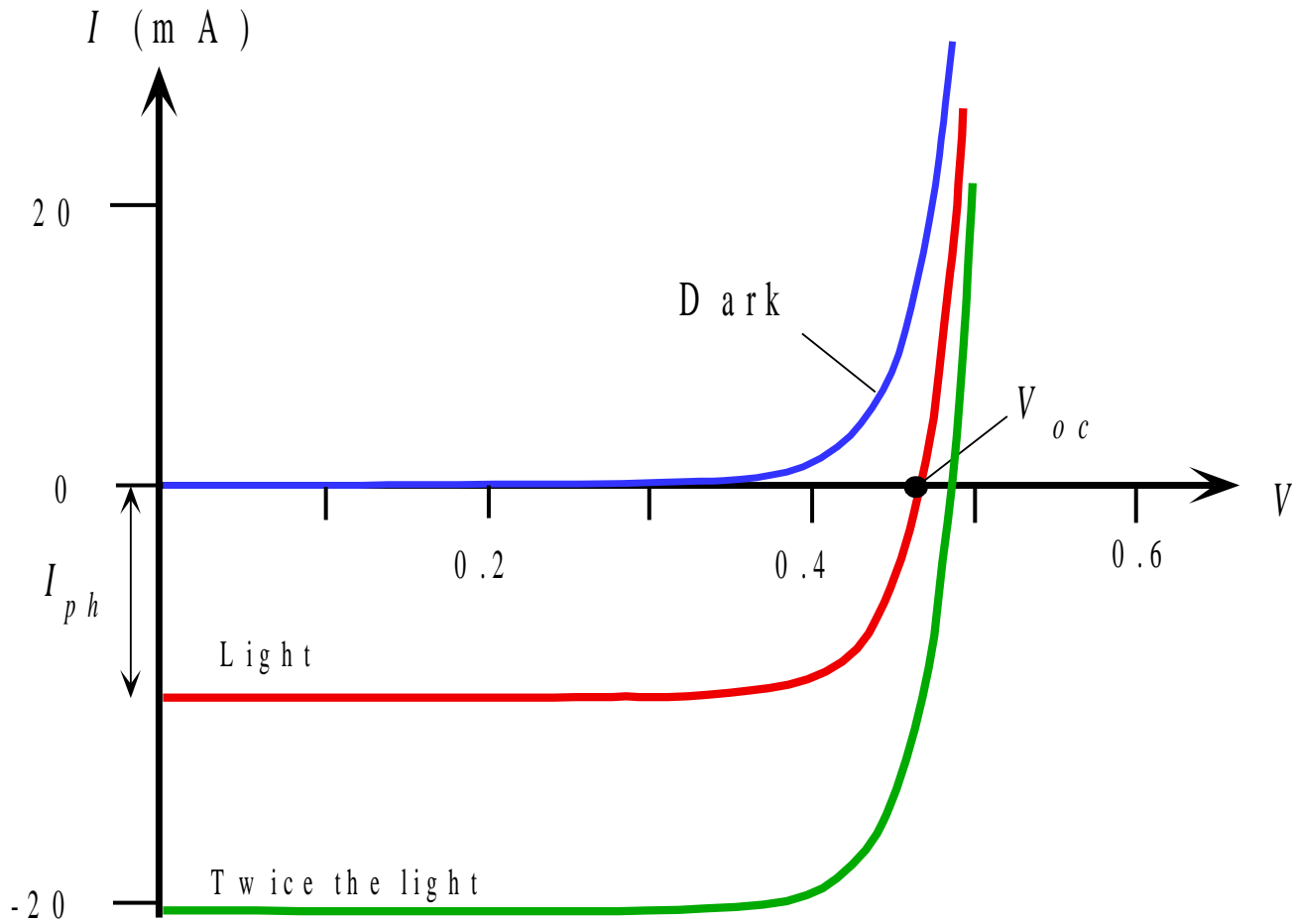
↖ ↘
Light intensity

↙
Constant that depends on the particular device

Solar cell I - V

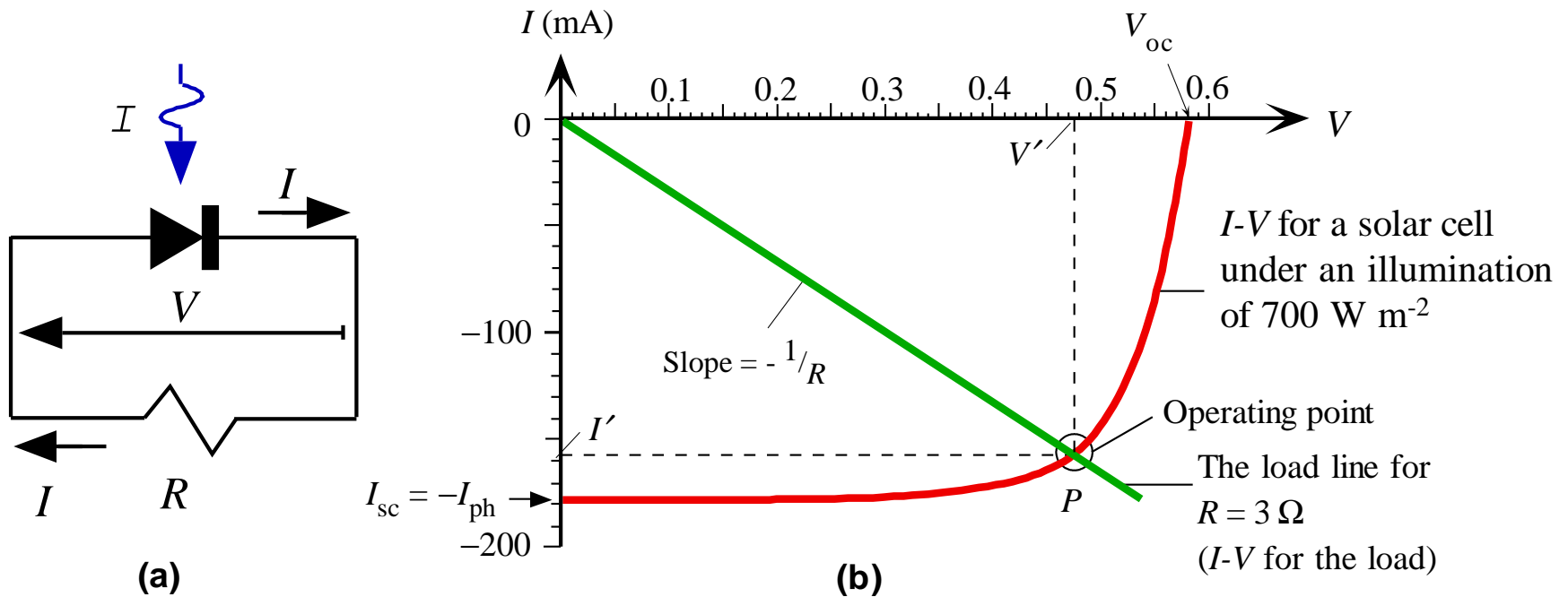
$$I = -I_{ph} + I_o \left[\exp\left(\frac{eV}{\eta kT}\right) - 1 \right]$$

where I_o is the reverse saturation current and η is the ideality factor: 1 - 2



Typical I - V characteristics of a Si solar cell. The short circuit current is I_{ph} and the open circuit voltage is V_{oc} . The I - V curves for positive current requires an external bias voltage. Photovoltaic operation is always in the negative current region

Fig 6.53



(a) When a solar cell drives a load R . R has the same voltage as the solar cell but the current through it is in the opposite direction to the convention that current flows from high to low potential. (b) The current I' and voltage V' in the circuit of (a) can be found from a load line construction. Point P is the operating point (I' , V'). The load line is for $R = 3 \Omega$.

Fig 6.54

Solar Cells

The load line

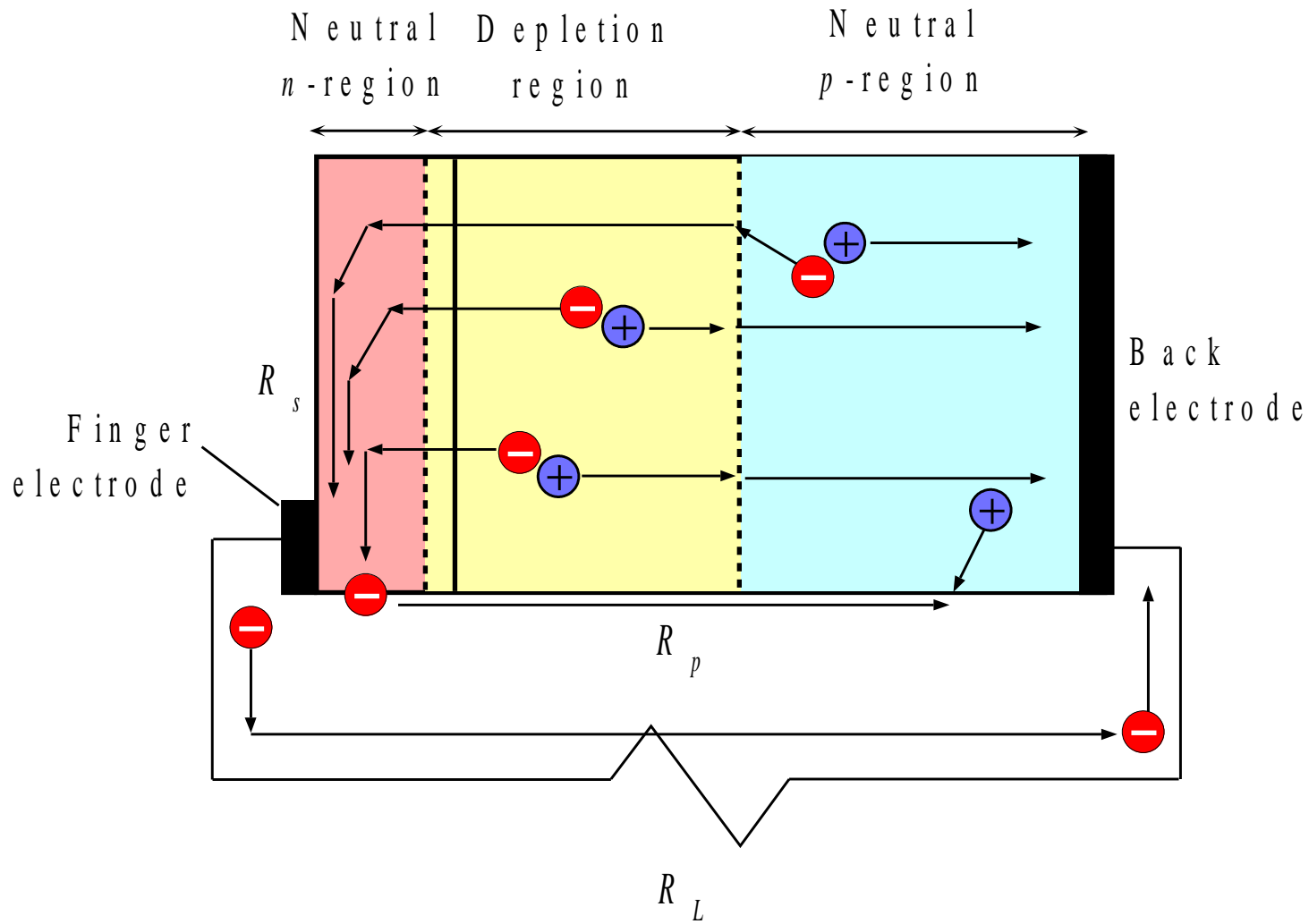
$$I = -\frac{V}{R}$$

The actual current I' and voltage V' in the circuit must satisfy both the $I - V$ characteristics of the solar cell and the load.

Definition of fill factor

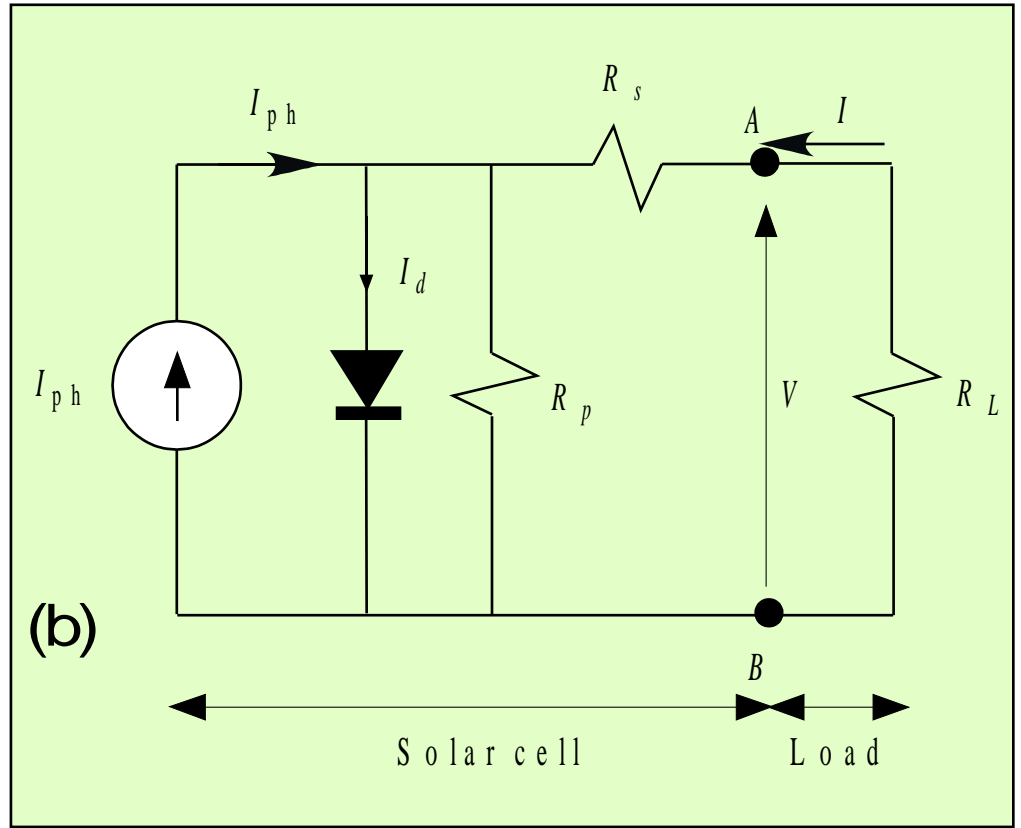
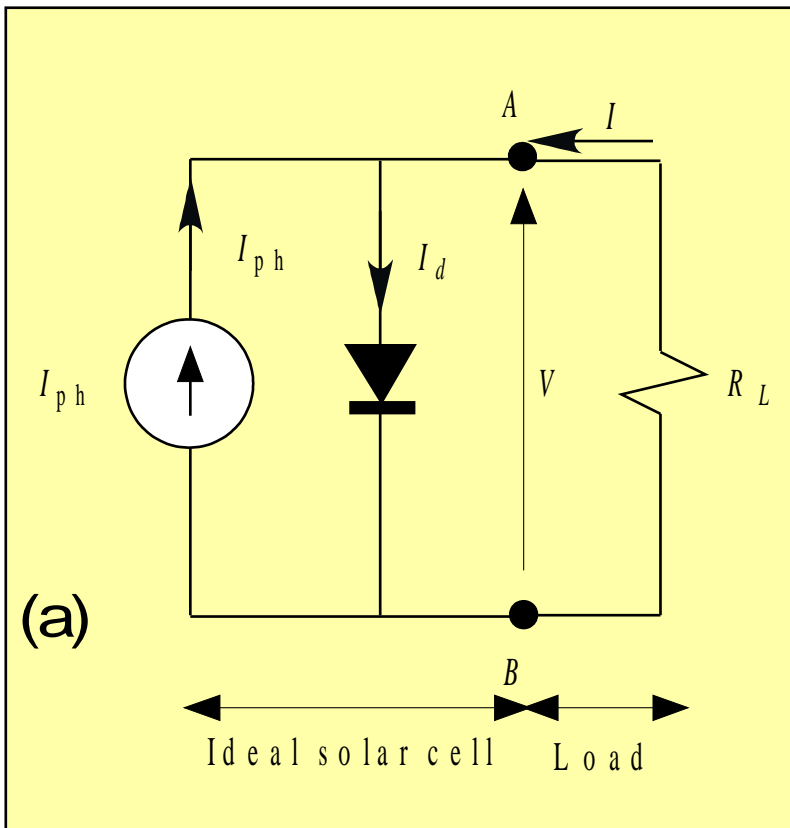
$$\text{FF} = \frac{I_m V_m}{I_{\text{sc}} V_{\text{oc}}}$$

The FF is a measure of the closeness of the solar cell $I-V$ curve to the rectangular shape (the ideal shape).



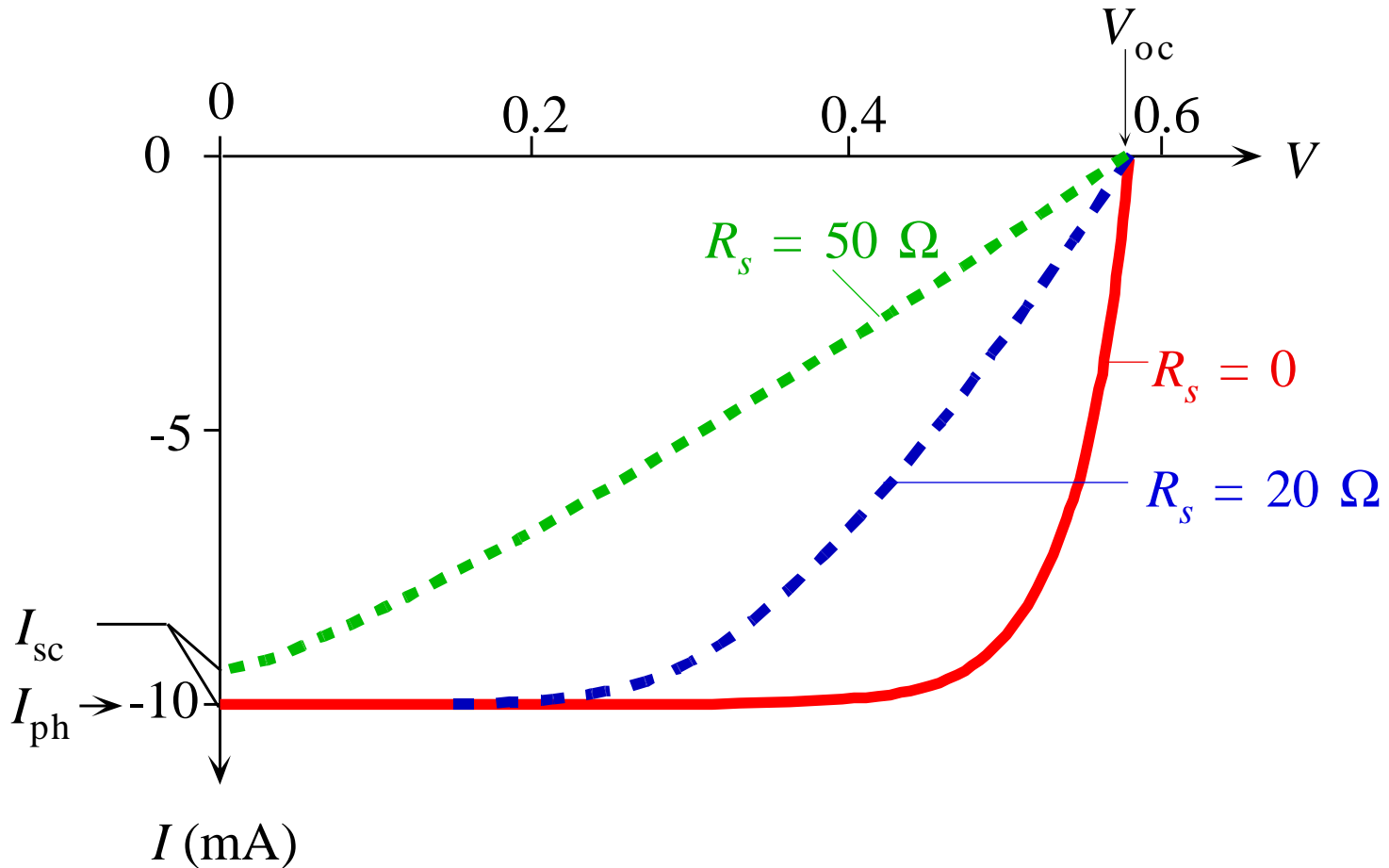
Series and shunt resistances and various fates of photogenerated EHPs.

Fig 6.55



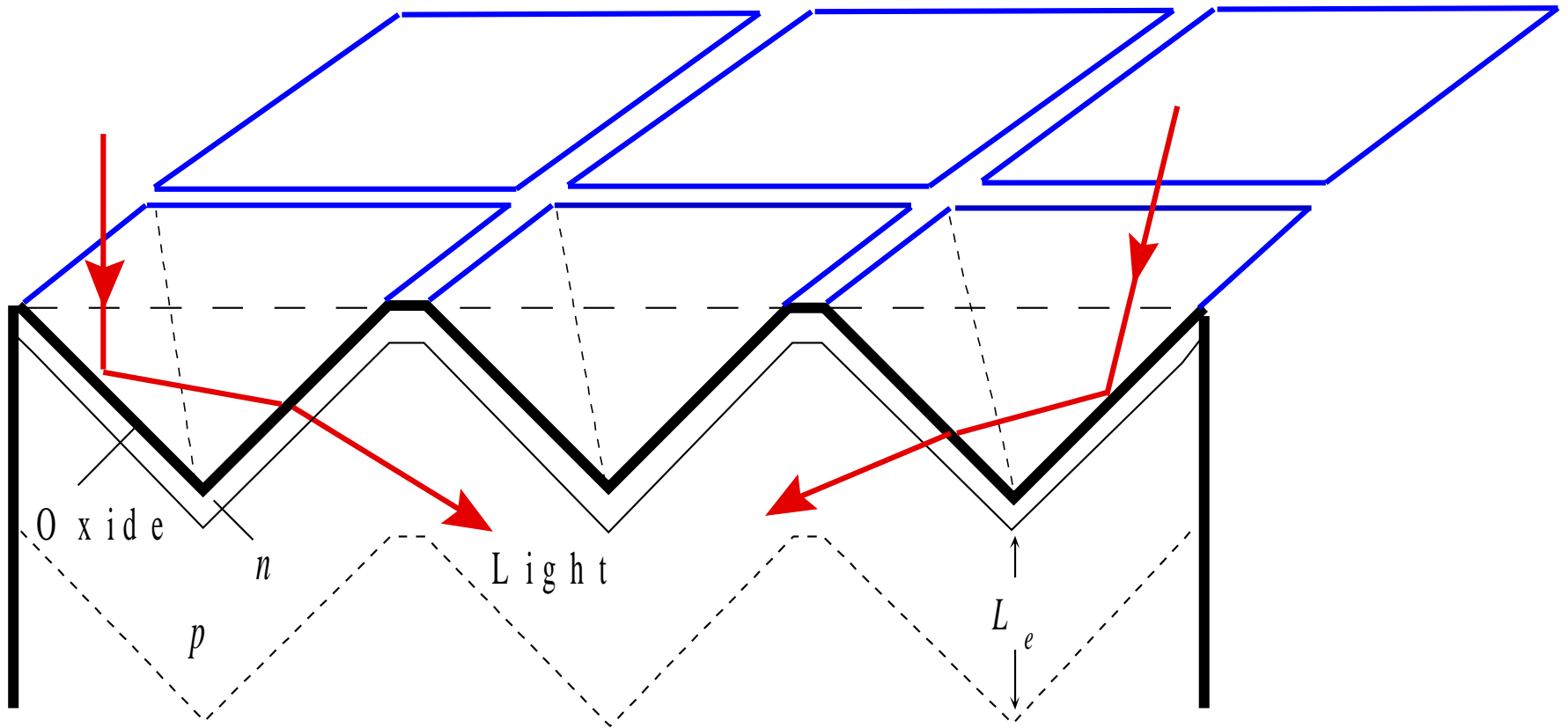
The equivalent circuit of a solar cell (a) Ideal pn junction solar cell
 (b) Parallel and series resistances R_s and R_p .

Fig 6.56



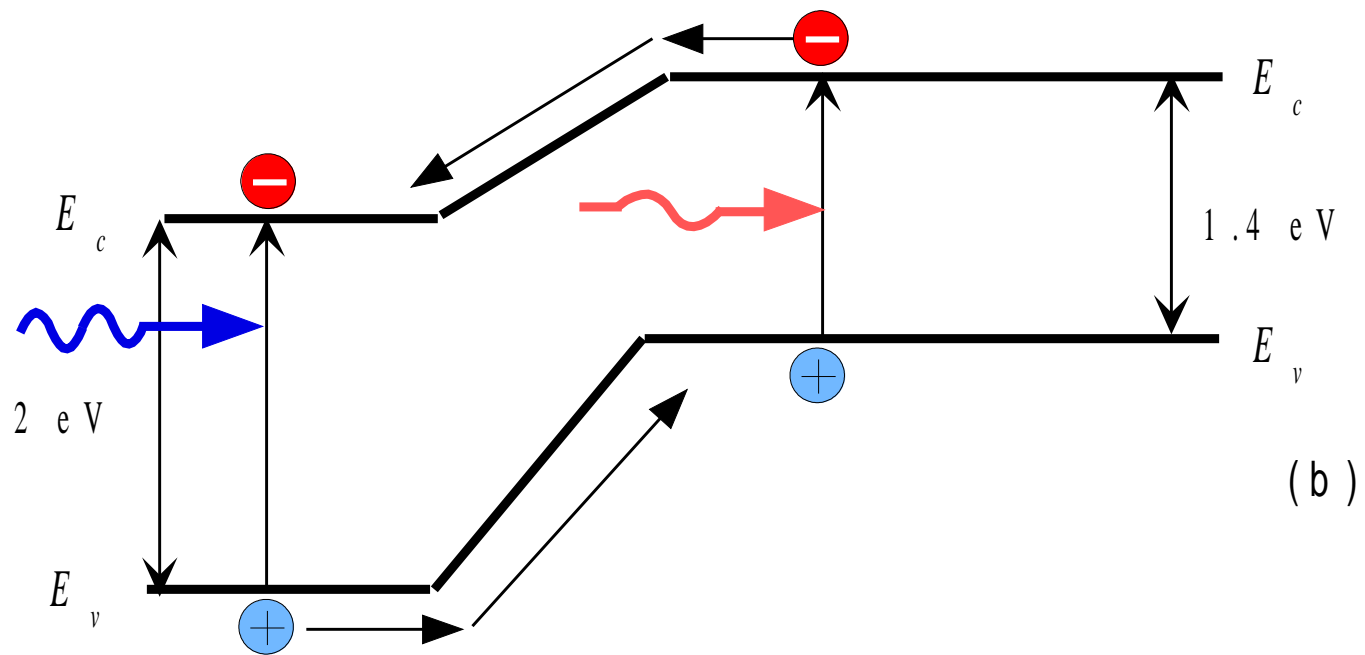
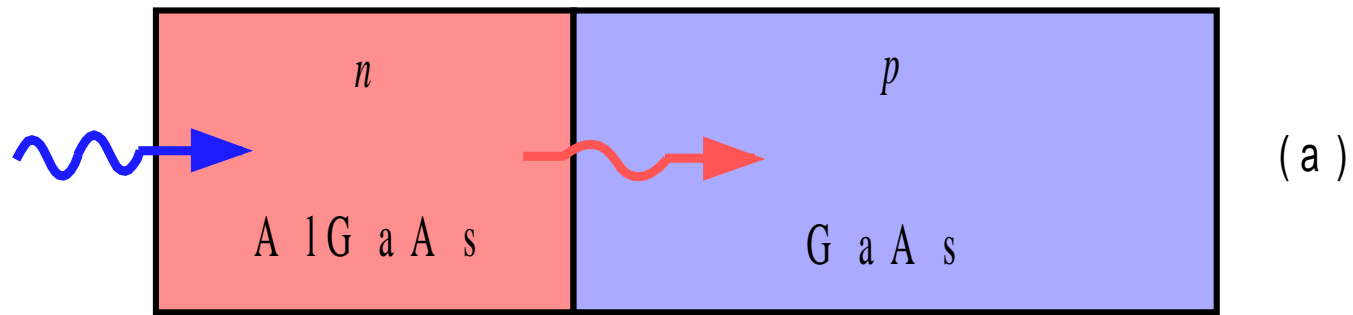
The series resistance broadens the I - V curve and reduces the maximum available power and hence the overall efficiency of the solar cell. The example is a Si solar cell with η 1.5 and

$I_o = 3 \times 10^{-6}$ mA. Illumination is such that the photocurrent $I_{ph} = 10$ mA.



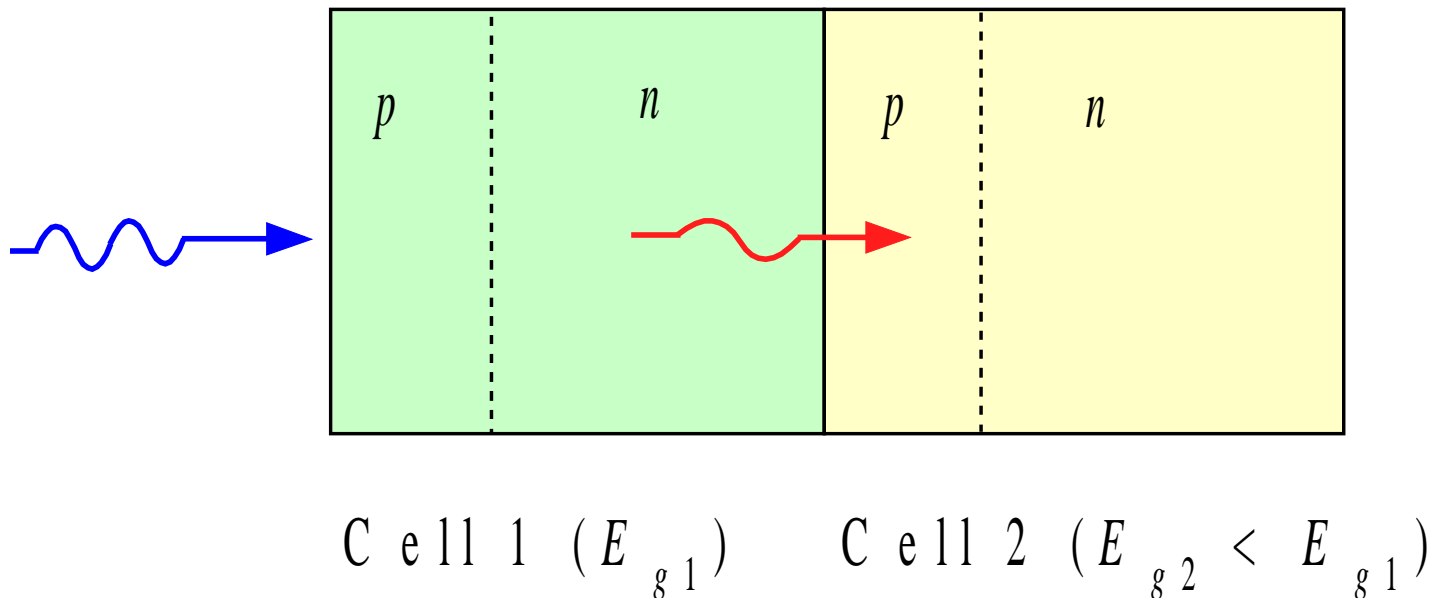
Inverted pyramid textured surface substantially reduces reflection losses and increases absorption probability in the device

Fig 6.58



A heterojunction solar cell between two different bandgap semiconductors (GaAs and AlGaAs)

Fig 6.60



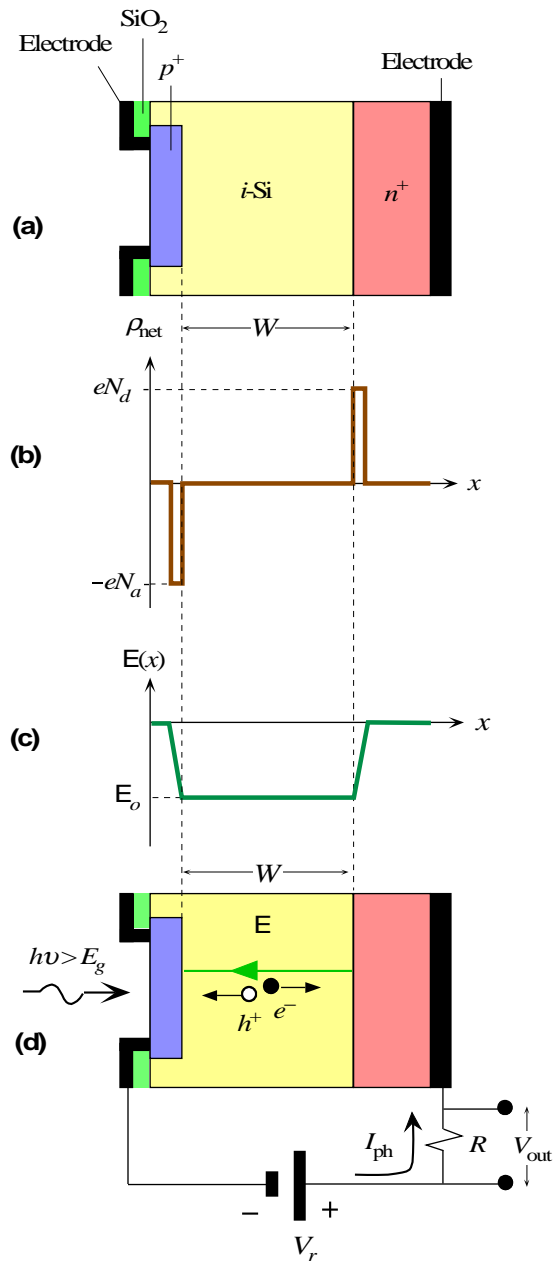
A tandem cell. Cell 1 has a wider bandgap and absorbs energetic photons with $h\nu > E_{g1}$. Cell 2 absorbs photons that pass cell 1 and have $h\nu > E_{g2}$.

Fig 6.61

PIN Diodes

- Optimized for speed/efficiency
- Intrinsic layer to enhance collection
- Speed determined by Cap.
- Reverse bias
 - Avalanche phenomena

Fig 6.61



(a) The schematic structure of an idealized *pin* photodiode (b) The net space charge density across the photodiode. (c) The built-in field across the diode. (d) The *pin* photodiode in photodetection is reverse biased.

Fig 6.62

pin Diodes, photodiodes and solar cells

Junction capacitance of *pin*

$$C_{\text{dep}} = \frac{\epsilon_o \epsilon_r A}{W}$$

where A is the cross-sectional area and $\epsilon_o \epsilon_r$ is the permittivity of the semiconductor (Si) and W is the width of the *i*-region.

Reverse biased *pin*: the electric field E in the *i*-region

$$E = E_o + \frac{V_r}{W} \approx \frac{V_r}{W} \quad (V_r \gg V_o)$$